Manuscript Number: MOLECULAR-CELL-D-09-00602R2

Title: Regulation of translesion synthesis DNA polymerase η by monoubiquitination

Article Type: Research Manuscript

Keywords: ubiquitin; monoubiquitination; polymerase eta; PCNA; translesion synthesis

Corresponding Author: Dr. Ivan Dikic,

Corresponding Author's Institution: Goethe University Medical School

First Author: Marzena Bienko

Order of Authors: Marzena Bienko; Catherine M Green; Simone Sabbioneda; Nicola Crosetto; Ivan Matic; Richard G Hibbert; Tihana Begovic; Atsuko Niimi; Matthias Mann; Alan R Lehmann; Ivan Dikic

Abstract: DNA polymerase η is a Y-family polymerase involved in translesion synthesis (TLS). Its action is initiated by simultaneous interaction between the PIP box in polη and PCNA, and between the UBZ in polη and monoubiquitin attached to PCNA. While monoubiquitination of PCNA is required for its interaction with polη during TLS, we now show that monoubiquitination of polη inhibits this interaction, preventing its functions in undamaged cells. Identification of monoubiquitination sites within polη nuclear localization signal (NLS) led to the discovery that polη NLS directly contacts PCNA, forming an extended polη-PCNA interaction surface. We name this region PIR (PCNA-Interacting Region) and show that its monoubiquitination is downregulated by various DNA-damaging agents. We propose that this mechanism ensures optimal availability of non-ubiquitinated, TLS-competent polη after DNA damage. Our work shows how monoubiquitination can either positively or negatively regulate the assembly of a protein complex depending on which substrates are targeted by ubiquitin.

Suggested Reviewers:

Opposed Reviewers:

Cover Letter

JOHANN WOLFGANG GOETHE
UNIVERSITÄT
FRANKFURT AM MAIN

University Hospital · Theodor-Stern-Kai 7 · 60590 Frankfurt

Dr. Feng Chen
Editor, Molecular Cell
600 Technology Square
Cambridge, MA 02139

Dear Feng,

we have revised our manuscript entitled: “Regulation of translesion synthesis DNA polymerase η by monoubiquitination” (MOLECULAR-CELL-D-09-00602R1) according to the editorial guidelines. We hope that it now meets all the requirements and is suitable for publication in Molecular Cell.

Sincerely,

Ivan Dikic

Institute for Biochemistry II
Ivan Dikic, MD, PhD
Professor of Biochemistry
e-mail: dikic@biochem2.de

Assistant: Rebecca Pfeiffer
Phone: 069/63 01-45 46
Fax: 069/63 01-55 77
e-mail: pfeiffer@biochem2.de
Homepage: www.biochem2.de

Date: 05.11.2009

Cardiovascular Signaling
W. Müller-Esterl, MD, PhD
M. Hoffmeister, PhD
St. Oess, PhD
A. Siehoff-Icking, PhD

Molecular Signaling
I. Dikic, MD, PhD
N. Crosetto, MD
C. Grabbe, PhD
K. Husnjak, PhD
F. Ikeda, DDM,PhD
Y. Lissanu Deribe MD
D. McEwan, PhD

Raft Signaling
R. Tikkanen, PhD
A. Banning, PhD

Cancer Cell Signaling
M. Innocenti, PhD
D. Xu, PhD

Emmy Noether Research Group
Cell Death Signaling
K. Rajalingam, PhD

Mailing address:
University Hospital, Bldg. 75
Theodor-Stern-Kai 7
60590 Frankfurt

Visiting address:
University Hospital, Bldg. 75
Sandhofstrasse 2 - 4
60598 Frankfurt

www.klinik.uni-frankfurt.de
Tramline: 15,19,21

***Response to reviewers**

No further issues were raised by the Reviewers.

Highlights

Polη is monoubiquitinated on one of four lysine residues, C-terminal to its UBZ domain. Three of these residues fall in the nuclear localization signal (NLS), while the fourth one is adjacent to the PIP box (PCNA-Interacting Peptide) motif.

The NLS of polη directly interacts with PCNA. Together with the PIP box, this NLS forms a PCNA-Interacting Region (PIR).

Monoubiquitination of the PIR inhibits the interaction of polη with PCNA and excludes the polymerase from the chromatin.

DNA damage causes de-ubiquitination of polη, allowing it to associate with monoubiquitinated PCNA at stalled replication forks.

Graphical Abstract

Click here to download Graphical Abstract: Graphical abstract.ai

Regulation of translesion synthesis DNA polymerase η by monoubiquitination

Marzena Bienko[1], Catherine M. Green[2,3#], Simone Sabbioneda[3#], Nicola Crosetto[1], Ivan Matic[4], Richard G. Hibbert[5], Tihana Begovic[1], Atsuko Niimi[3], Matthias Mann[4], Alan R. Lehmann[3*], Ivan Dikic[1*]

[1]Institute of Biochemistry II, Goethe University Medical School, Theodor-Stern-Kai 7, D-60590 Frankfurt am Main, Germany

[2]Department of Zoology, University of Cambridge, Downing Street, Cambridge CB2 3EJ, UK

[3]Genome Damage and Stability, University of Sussex, Falmer, Brighton BN1 9RQ, UK

[4]Department of Proteomics and Signal Transduction, Max Planck Institute for Biochemistry, Am Klopferspitz 18, D-82152 Martinsried, Germany

[5]Molecular Carcinogenesis and Center for Biomedical Genetics, The Nederlands Cancer Institute, Plesmanlaan 121, 1066 CX Amsterdam, The Nederlands

[#] These Authors contributed equally to this work.

[*]Correspondence: ivan.dikic@biochem2.de (I.D.), a.r.lehmann@sussex.ac.uk (A.R.L.)

Running title: Ubiquitination of DNA polymerase η

Abstract

DNA polymerase η is a Y-family polymerase involved in translesion synthesis (TLS). Its action is initiated by simultaneous interaction between the PIP box in polη and PCNA, and between the UBZ in polη and monoubiquitin attached to PCNA. While monoubiquitination of PCNA is required for its interaction with polη during TLS, we now show that monoubiquitination of polη inhibits this interaction, preventing its functions in undamaged cells. Identification of monoubiquitination sites within polη nuclear localization signal (NLS) led to the discovery that polη NLS directly contacts PCNA, forming an extended polη-PCNA interaction surface. We name this region PIR (PCNA-Interacting Region) and show that its monoubiquitination is downregulated by various DNA-damaging agents. We propose that this mechanism ensures optimal availability of non-ubiquitinated, TLS-competent polη after DNA damage. Our work shows how monoubiquitination can either positively or negatively regulate the assembly of a protein complex depending on which substrates are targeted by ubiquitin.

Introduction

Most types of DNA damage block the progression of replication forks, because replicative DNA polymerases cannot accommodate damaged bases in their active sites. One way in which cells deal with this problem is by employing a specialised set of DNA polymerases that carry out translesion synthesis (TLS) past DNA lesions (Friedberg et al., 2005). These polymerases, mostly belonging to the Y-family, have a more open conformation and can accommodate different damaged bases in their active sites (Yang and Woodgate, 2007). The active sites in the Y-family are conserved between different family members and are typically contained within the N-terminal 450 amino acids. In contrast, the 250-400 C-terminal amino acids are poorly conserved and are not required for catalytic activity. Instead, this region mediates interactions between Y-family polymerases and other proteins, and contains sequences required for their sub-nuclear localisation (Guo et al., 2003; Kannouche et al., 2001; Kannouche et al., 2003; Ogi et al., 2005). In eukaryotes, the Y-family DNA polymerase η can replicate with equal efficiency past undamaged thymines and past the major UV photo-product, the thymine-thymine cyclobutane pyrimidine dimer (McCulloch et al., 2004). In humans, the lack of polη causes the variant form of the skin cancer-prone syndrome xeroderma pigmentosum (XPV) (Johnson et al., 1999; Masutani et al., 1999). Typically, cells from these individuals are defective in replicating DNA past UV photoproducts (Lehmann et al., 1975).

Ubiquitin represents a signalling molecule, which cells use as a versatile tool to properly respond to both environmental and intracellular stimuli. Ubiquitination has been implicated in processes such as proteasomal degradation, endocytosis, autophagy, chromatin remodelling and DNA repair (Bennett and Harper, 2008; Finley, 2009; Haglund and Dikic, 2005; Hicke, 2001; Kirkin et al., 2009; Mukhopadhyay and Riezman, 2007). This is mediated by specialized domains, called Ub-binding domains (UBDs) embedded in various proteins, which non-covalently interact with Ub-conjugated substrates (Dikic et al., 2009; Hurley et al., 2006). For instance, UBD-Ub interactions have been shown to mediate the "polymerase switch", a term which refers to the replacement of stalled replicative polymerases with specialized TLS polymerases upon stalling of the replication machinery at sites of DNA damage (Friedberg et al., 2005). When a DNA lesion or depletion of the deoxyribonucleotide pool blocks the replication machinery, this triggers monoubiquitination of PCNA at lysine 164 (Hoege et al., 2002). In *Saccharomyces cerevisiae* and human cells, this reaction is brought about by the E2 ubiquitin conjugating enzyme Rad6 and the E3 ubiquitin ligase

Rad18 (Hoege et al., 2002; Kannouche and Lehmann, 2004; Koken et al., 1991; Tateishi et al., 2000; Watanabe et al., 2004). Compared to the unmodified form, monoubiquitinated PCNA has increased affinity for polη (Bienko et al., 2005; Garg and Burgers, 2005; Kannouche et al., 2004; Plosky et al., 2006; Watanabe et al., 2004). Biochemical and computational studies have revealed that all the members of the human Y-family, polη, polι, polκ and Rev1 contain UBDs located in their C-terminal regions (Bienko et al., 2005). We have previously designated these domains UBM for Ub-Binding Motif (polι and Rev1) and UBZ for Ub-Binding Zinc-finger (polη and polκ). Several studies have addressed the function of UBDs in Y-family polymerases at the onset of TLS (Bienko et al., 2005; Garg and Burgers, 2005; Guo et al., 2008; Guo et al., 2006; Plosky et al., 2006; Sabbioneda et al., 2008; Sabbioneda et al., 2009).

We previously showed that a fraction of polη is monoubiquitinated in human cells (Bienko et al., 2005). In the current work we have identified lysines in the nuclear localization signal (NLS) as sites of ubiquitination of polη. This in turn led to the discovery that the NLS is involved in direct binding to PCNA and that this interaction is disrupted by monoubiquitination. In addition we show how this modification is affected by DNA damage, and how different motifs in the extreme C-terminus of polη influence the response of cells to UV-induced damage.

Results

Identification of monoubiquitination sites in polη

In the course of our previous work, we observed a minor species of over-expressed human polη with reduced mobility in SDS-PAGE, and showed that this corresponds to the ubiquitinated form of the polymerase (Bienko et al., 2005). Mutant forms of polη carrying mutations in the UBZ domain did not undergo ubiquitination, proving the UBD-dependence of this modification (Bienko et al., 2005). Interestingly, a genetic in-frame fusion of polη with Ub bound much less potently to ubiquitin in comparison to wild-type polη. We hypothesized that this was the result of an intramolecular interaction between the UBZ of polη and the Ub moiety fused to it, as also shown for other UBD-containing proteins fused to Ub (Hoeller et al., 2006). Following this work, we have sought to characterize the mechanism and the role of polη ubiquitination in detail.

Accordingly, in MRC5 cells we were able to detect a form of endogenous polη of reduced mobility in SDS-PAGE that we presumed to be monoubiquitinated polη (Figure 1A). This band was absent in polη-deficient XP30RO cells (Figure 1A), demonstrating that it is indeed a species of polη. Moreover, a corresponding band did contain monoubiquitinated polη when excised from a Coomassie blue-stained gel and analysed by mass spectrometry (see below).

We next attempted to identify the lysine residue(s) in polη that can be ubiquitinated. HEK293T cells were transfected with HA-tagged ubiquitin and Flag-tagged polη. After immunoprecipitation of polη with anti-Flag antibodies, the presumptive monoubiquitinated species of polη was visualized by Coomassie blue stain and excised from the gel (data not shown). Mass spectrometry of the isolated protein revealed a major ubiquitinated species at lysine 682 (K682), which lies in the first segment of the bipartite NLS (Figure S1A and Figure 1C). However polη carrying a mutation of this lysine (K682R) was still modified (Figure 1B). A further round of mass spectrometry using polη-K682R revealed a second ubiquitination site at lysine 709, but a double mutant again did not show a major decrease in its monoubiquitination status (Figure 1B). Interestingly, both lysine residues lie in a short fragment C-terminal to the UBZ domain, which overall contains four lysine residues (K682, K686, K694, K709) (Figure 1C). Thus, we hypothesized that this is the region where ubiquitin can be attached under physiological conditions. We reasoned that if the prevalent ubiquitination site lysine 682 is mutated, the lysine residues adjacent to it may become targeted. Indeed, when all these four lysine residues were mutated to arginines (polη4K/R), no ubiquitinated species of polη was detectable (Figure 1B) under various lysis conditions (Figure S1B). Interestingly, three out of four of these lysine residues are part of the bipartite NLS of polη and are well conserved from mammals down to amphibians (Figure 1C). The attachment of Ub to this region could be recapitulated *in vitro* and occurred in the absence of any E3 ligase, confirming our previous finding that certain UBDs can directly mediate ubiquitination of their host proteins by binding to the E2-Ub complex (Figure S1C) (Hoeller et al., 2006; Hoeller et al., 2007).

To gain further insight into the function of polη NLS and its ubiquitination we created a panel of EGFP-tagged full-length polη expression constructs, as pictured in Figure 1D. Since three out of four residues mutated in polη4K/R lie within the NLS sequence of polη, we tested whether the observed loss of monoubiquitination resulted from inefficient nuclear localization. We noted that, in contrast to wild-type polη, we could detect a significant

fraction of polη4K/R in the cytoplasm (Figure 1E, bottom left), which was most obvious in non-S phase cells (Figure S1D). In order to ensure that this altered localization would not interfere with subsequent interpretation of our data, we introduced an exogenous NLS into several expression constructs N-terminal to EGFP (Figure 1D). After insertion of the NLS sequence of the SV40 large T antigen into EGFP-polη4K/R (NLS-EGFP-polη4K/R), this mutant became exclusively nuclear (Figure 1E, bottom right). Importantly, this protein was still not monoubiquitinated, in contrast to wild-type NLS-EGFP-polη (Figure S1E). Moreover, mutation of arginines 683, 695 and 696 in the NLS to alanines (polη3R/A) had no effect on ubiquitination (Figure S1E), demonstrating that the observed lack of ubiquitination in polη3K/R or polη4K/R is not a secondary effect of mutating basic residues in the NLS.

Monoubiquitination of polη is dependent on its UBZ motif (Bienko et al., 2005). In order to prove that the aforementioned lysine residues are sites of monoubiquitination, we needed to exclude the possibility that polη4K/R is not monoubiquitinated because of its inability to bind ubiquitin. In fact, the UBZ domain of polη4K/R was functional as its binding to Ub was similar to that of wild-type polη (Figure S2A). We conclude that monoubiquitination of polη occurs C-terminal to its UBZ domain, at one of the four lysine residues available in this region.

The NLS of polη is a PCNA-interacting surface

Since monoubiquitination sites in polη lie in a regulatory region known to be involved in protein-protein interactions (Bienko et al., 2005; Plosky et al., 2006), we hypothesized that this modification could be involved in the regulation of polη interactions with other proteins. Since three out of four monoubiquitination sites are in the NLS sequence, we focused on finding interacting partners of this region. For this purpose we used the yeast two-hybrid system to screen a human spleen cDNA library with the last 112 amino acids of polη as bait. Proteins found in the screen (Table S1) were probed for their ability to interact with a mutant of polη in which all the positively charged residues in the NLS were substituted by alanines (NLS*). Importin alpha 1, one of the clones found in the screen, which is known to mediate the nuclear import of many proteins upon recognition of their NLS (Chook and Blobel, 2001), did not interact with polηNLS* (Figure S2B). To our surprise, PCNA was also unable to interact with this mutant (Figure S2B). Previous studies (Haracska et al., 2001; Kannouche et al., 2004) have mapped the PCNA-interaction site in polη to amino acids 702-708 which form the PIP box motif found in many other PCNA-interacting proteins (Maga and Hubscher,

2003). As shown in Figure 2A, mutation of either NLS (NLS*) or PIP (L704A, F707A, F708A; PIP*) abolished the interaction of polη with PCNA, leading us to hypothesize that the PIP box is not the only motif in polη that can directly contact PCNA.

To verify this hypothesis, several GST pull-down experiments were performed. Firstly, we tested whether GST fusions of the C-terminal portion of polη containing the UBZ domain, NLS and PIP box (amino acids 602-713, GST-polη_C) were able to interact with recombinant PCNA. Interestingly, while GST-polη_CWT effectively captured PCNA, a decrease in the strength of this interaction was observed depending on how many positive charges in the NLS were mutated to alanines (Figure 2B). Mutation of all lysines to alanines (GST-polη_C3K/A) strongly reduced binding (lane 4), though not as much as mutation of all lysines and arginines (GST-polη_CNLS*) (lane 5). Mutation of the PIP box (GST-polη_CPIP*) compromised binding to PCNA similarly to GST-polη_CNLS* (lane 6). Notably, mutation of all lysines in the NLS to arginines (GST-polη_C3K/R) did not influence the polη-PCNA interaction, while additional mutation of lysine 709 (GST-polη_C4K/R) slightly decreased it (lanes 7, 8). The observed interaction between GST-polη_CWT and PCNA could be easily titrated and was still detectable at a PCNA concentration of around 30 nM (Figure 2C). In contrast, both GST-polη_CNLS* and GST-polη_CPIP* barely captured PCNA at a concentration of 600 nM (Figure 2C).

We next checked whether polη NLS mutations influence its interaction with PCNA in cell lysates. For this purpose, we used HEK293T cells over-expressing various EGFP-polη constructs and tried to pull them down with GST-PCNA (Figure 2D). Wild-type polη effectively bound PCNA (lane 2) while mutations in either the NLS or PIP decreased the interaction (lanes 3, 4, 7). Notably, only mutations that changed the positive charge in the NLS (as in the case of polηNLS*) had a substantial influence on the polη-PCNA interaction, to a similar extent as the PIP box mutation. The polη3K/R mutant bound to PCNA as potently as the wild-type protein (lane 5), while the interaction of polη4K/R with PCNA was slightly weaker than polη3K/R (lane 6). Again, mutation of only lysine residues to alanines (polη3K/A) exerted an intermediate influence on the strength of the polη-PCNA interaction, between that of wild-type and polηNLS* (lane 7). Interestingly, as in Figure 2C, polηNLS* and polηPIP* still displayed residual interaction with PCNA (Figure 2D). Altogether, these data indicate that positive charges in the NLS of polη are important for its direct interaction with PCNA, while the contribution of the region containing the PIP box seems more stringently dependent on its full primary sequence, as mutation of lysine 709 already weakens

this interaction. This also implies that K709 is involved in the binding of polη to PCNA. Indeed, this residue was recently shown to directly contact PCNA in the crystal structure of this protein with a peptide comprising residues 694-713 of polη (Hishiki et al., 2009). Additionally, the same work showed that residues 710-713 are important to stabilize the interaction between K709 of polη and G127 of PCNA. From now on, we will refer to the surface of polη containing amino acids 682-713 as the PCNA-Interacting Region (PIR).

The PCNA-Interacting Region (PIR) in polη regulates its sub-nuclear localization and is important for DNA damage tolerance

We next explored the function of polη PIR *in vivo*. Firstly, we used confocal microscopy to quantify the amount of cells containing EGFP-polη foci after expression of various constructs in MRC5 cells. In order to limit our analysis to the influence of the NLS on polη sub-nuclear localization, we used the constructs containing the additional NLS from the SV40 large T antigen. Mutation of lysines in the NLS to arginines did not change the localization pattern of polη (Figure 1E and Figure 3B). NLS-EGFP-polη3K/R formed foci in approximately 20% of cells, exactly like the wild-type counterpart. In striking contrast, when a corresponding alanine mutant of the NLS (NLS-EGFP-polη3K/A) was tested, the number of cells with polη foci dropped from 22% to 5%. Moreover, the NLS-EGFP-polη3R/A construct, which could still undergo monoubiquitination as efficiently as the wild-type protein (Figure S1E) behaved very similarly to NLS-EGFP-polη3K/A in terms of the localization (Figure 3B). In order to see an almost complete loss of polη foci we needed to mutate all the positive charges of the NLS to alanines (NLS-EGFP-polηNLS*) (Figure 3A and B). This behaviour matched the results of the above polη-PCNA interaction studies. The drop in the percentage of cells with polη foci mirrored the decrease seen in polη-PCNA binding strength for different mutants of the NLS (Figure 2). The localization of polη in foci depended on its interaction with PCNA and indeed polηPIP* did not accumulate in replication foci in any cell (Figure 3B) as also reported for BL2 cells (Gueranger et al., 2008). These results reveal that the NLS sequence in polη not only constitutes a classical signal for nuclear import, but is also required for its physiological sub-nuclear distribution.

Having found that the whole NLS-PIP region in polη is needed for its presence inside replication foci, presumably by mediating a direct interaction with PCNA, we wondered how this might translate into the ability of polη to by-pass DNA damage. For this purpose, we generated a set of stable XP30RO cell lines expressing various mutants of EGFP-polη and

compared them in a clonogenic UV survival assay. We analyzed mutants of all the known interaction surfaces important for the binding of polη to monoubiquitinated PCNA. All the cell lines reconstituted with mutants (UBZ*, NLS* or PIP*) displayed significantly lower survival, when compared to XP30RO cells complemented with wild-type polη (Figure 3C and Table S2). Importantly, the effects observed from mutating the NLS of polη were not restricted only to point mutations of the NLS. In parallel we have been studying a second NLS mutant in which the whole of the NLS was deleted (ΔNLS). The ΔNLS mutant also showed inability to accumulate in replication foci and was impaired in its interaction with PCNA, similarly to the NLS* (data not shown). We used this mutant to study the effect of simultaneous inactivation of both the UBZ and the PIR. Both double mutants (UBZ*/ΔNLS and UBZ*/PIP*) failed to restore UV survival of XP30RO cells to a significantly larger extent than any of the single mutants (Figure 3C). This synergistic effect demonstrates that the individual motifs co-operate to provide a fully functional polη.

To gain further insight into the importance of these motifs, we also analysed the ability of the same mutants to restore post-replication repair (PRR) activity in XP30RO cells after UV irradiation, by measuring the size of newly synthesised DNA strands on alkaline sucrose gradients. XPV cells have a pronounced deficiency in this process, so that under a set of standard conditions, the size of the newly synthesised DNA in irradiated XPV cells is much smaller than that of wild-type cells (Lehmann et al., 1975). This deficiency is rescued with wild-type EGFP-polη (Figure 3D). Consistent with the survival data, we found that the rescue of PRR was reduced in all the mutants tested, and was reduced more in the double than the single mutants (Figure 3D). There was a good correlation between the defects in PRR and the UV sensitivities.

Finally, we investigated how the PIR-mediated polη-PCNA interaction influences the kinetics of cell proliferation after UV irradiation. For this purpose, we applied a technology that records the collective behaviour of cell populations in real-time (xCelligence, Roche). This system monitors the electric impedance of cells grown in a 96-well plate and can provide information about the cellular response to UV starting from early times after irradiation. Cells complemented with either wild-type polη, PIP* or NLS* mutants, but not with empty vector, underwent a delayed recovery phase after an apparent exponential decay phase (Figure 3E and S3B). In the case of wild-type polη-complemented cells the decay was shorter and the recovery occurred sooner as compared to cells expressing mutants of polη (Figure 3E and Table S3). In all the cases, the recovery phase could be accurately modelled

by the Boltzmann´s sigmoid equation. Simultaneous monitoring of non-irradiated cells allowed for accurate correction for differences coming from different cell lines that were polη-independent (data not shown). The relative outgrowths of the surviving cells at later times corresponded well with the relative survivals predicted from the clonogenic assay (Table S2 and S3). Interestingly, increasing the caffeine concentration from 0.4 to 0.8 mM resulted in greater discrimination between wild-type and PIP* or NLS* cell lines (Figure S3A). Altogether, these data indicate that the PIR region in polη is important for DNA damage tolerance, and cast light on the real-time dynamics of this process at a population level.

Monoubiquitination of polη masks its PCNA-Interacting Region (PIR)

Attachment of Ub to the PIR in polη could exert a dual effect. Because target lysines are relatively near to the UBZ domain, an intramolecular interaction between Ub and UBZ could take place, as previously described for other UBD-containing proteins (Hoeller et al., 2006). In turn, this could block the UBZ and additionally change the conformation of the entire region between the UBZ and the ubiquitinated lysine, making this surface inaccessible.

To clarify these issues we took advantage of a polη-Ub chimera that we had engineered by genetically fusing one Ub moiety to the C-terminus of polη (Bienko et al., 2005). Such a polη-Ub fusion as well as other chimeras previously generated in our group by fusing ubiquitin to UBD-containing proteins (Hoeller et al., 2006) have limited ability to interact with ubiquitin, probably because the UBD is engaged in a strong intramolecular interaction with Ub *in cis* (Figure 4A) (Bienko et al., 2005; Hoeller et al., 2006). In the case of polη, because its ubiquitination can occur as close as four amino acids from the C-terminus, this chimera is expected to be a good mimic for the *in vivo* effects of monoubiquitination of polη. When expressed in MRC5 cells, EGFP-polη-Ub was found in replication foci less frequently than EGFP-polη. Indeed, the percentage of cells displaying polη foci dropped from 22% for wild-type EGFP-polη down to 6% for the chimera (Figure 4B and C). Mutation of I44 in Ub, known to abolish its interaction with the UBZ of polη (Bomar et al., 2007), restored the sub-nuclear pattern of the chimera (Figure 4C), indicating that in EGFP-polη-Ub the Ub moiety is engaged in interaction with the UBZ domain. Consistent with these findings, we were unable to detect the ubiquitinated form of polη in the cellular Triton X-100-resistant fraction, which corresponds to the microscopically visible focal fraction of polη as we have previously demonstrated (Figure 4D and S4) (Kannouche et al., 2004).

We then wondered whether the exclusion of polη-Ub from foci results from deficient interaction with PCNA. Indeed, EGFP-polη-Ub displayed a lower affinity for GST-PCNA in a pull-down test, in comparison with the wild-type counterpart (Figure 4E). This reduction resembled the one observed for the polηNLS* and polηPIP* mutants (Figure 2D). We conclude that attachment of Ub at the C-terminus of polη weakens its interaction with PCNA.

Lastly, we used the same chimera as a model to study how monoubiquitination affects the ability of polη to mediate TLS. XP30RO cell lines stably expressing EGFP-polη-Ub were used both in clonogenic and PRR assays. Similar to the PIR mutants, cells reconstituted with the chimera displayed a significantly lower ability to tolerate UV and perform PRR in comparison to wild-type polη-expressing cells (Figure 4F and G and Table S3). Altogether, these data indicate that, *in vivo*, monoubiquitination of polη might negatively regulate its activity in translesion DNA synthesis.

DNA-damaging agents that trigger TLS inhibit monoubiquitination of polη

Since the various motifs in polη that are likely masked by ubiquitination (UBZ, NLS, PIP) are important for DNA damage tolerance (Figure 3), we decided to investigate the fate of ubiquitinated polη after exposure to various DNA-damaging agents. Remarkably, a decrease in ubiquitination of polη was visible following UV irradiation. This was seen either as a dose-response 6 hours after irradiation, or as a time-dependent decay following 30 J/m^2 UV irradiation (Figure 5A). A similar decrease was observed following treatment with the cross-linking agent cisplatin, but not with its inactive analogue transplatin (Figure 5B). Methyl methanesulfonate (MMS) also reduced the amount of monoubiquitinated polη (Figure 5B). Interestingly, exposure to hydroxyurea (HU) for up to twenty-four hours, which results in stalling of replication forks by depletion of the deoxyribonucleotides but does not generate DNA damage, had no impact on polη ubiquitination (Figure 5B). These data demonstrate that agents causing DNA lesions that can be processed by TLS simultaneously deplete the fraction of monoubiquitinated polη, possibly increasing the local pool of polη capable of interacting with PCNA.

Discussion

When we previously described the presence of Ub-binding domains (UBD) in Y- family polymerases, we also noted that a fraction of each polymerase was ubiquitinated in a UBD-dependent manner. We have now addressed the issue of which lysine residues are targeted by

this modification in polη and what its function is. To date there is a limited number of studies mapping ubiquitination sites in proteins, especially UBD-containing ones. Such searches have been compromised by the lack of a consensus sequence. In the present study we find that mutation of the residue in polη initially identified as being monoubiquitinated (K682), did not abrogate this modification, as neighbouring lysines would eventually become targeted. Only a simultaneous mutation of all the four lysines C-terminal to the UBZ motif abolished this modification completely. The fact that UBDs are directly engaged in mediating ubiquitination (Hoeller et al., 2007; Woelk et al., 2006) might make a difference in the choice of the target residue(s) for monoubiquitination in comparison to proteins without such domains. In the situation in which the output of monoubiquitination is an intramolecular interaction between Ub and a UBD, it might not be crucial that a specific residue is modified by Ub but rather that a certain region of a protein is modified. Our study on monoubiquitination of polη might be a good example of such a scenario. We hypothesize that an intramolecular interaction between the UBZ and Ub attached to the C-terminal part of polη will have the same result independently of which lysine in the C-terminus of polη is modified.

We find that three out of four ubiquitination sites in polη are present in its NLS. By addressing the function of this modification we discovered that this NLS belongs to a broader PCNA-interaction surface, which we name PIR. This seems to be a more general phenomenon, as we found a similar situation with polκ, which also has a juxtaposition of NLS and PIP box (Figure S5A). Indeed, mutation of polκ NLS interfered with its binding to PCNA (data not shown). Interestingly, crystal structures of PCNA with p21 and Fen1 – both of which carry PIP box motifs – show that the surface of interaction with PCNA is broader than the PIP box itself and also includes amino acids of their bipartite NLS sequences (Gulbis et al., 1996; Sakurai et al., 2005). In the case of p21, the PIP box motif lies in between the two parts of the bipartite NLS sequence (Gulbis et al., 1996), while in Fen1 the NLS is positioned C-terminal to the PIP box (Figure S5A). The different arrangement of PIP and NLS within the PIR of these proteins is likely to impact upon their affinity for PCNA. The importance of residues outside of the PIP box for mediating PCNA interactions is also highlighted by a recent study where PCNA could be co-crystallized with the PIP box of polη but failed to do so with the PIP of polκ unless additional residues were added (Hishiki et al., 2009).

We have previously characterized two motifs in polη important for its proper function in TLS, namely the UBZ domain and the PIP box, and showed that they are involved in direct interaction with monoubiquitinated PCNA. We now add the NLS to the list of motifs important for polη function in TLS, not only as a direct binding surface but also as a regulatory part controlling the interaction between polη and PCNA. The latter could be achieved by cycles of monoubiquitination and deubiquitination of the NLS. We propose that for polη to efficiently bind monoubiquitinated PCNA during TLS, all the three regions (UBZ, NLS and PIP box) must be available. Indeed, mutation of any of them diminished the ability of the cells to generate intact daughter DNA strands after UV-irradiation (PRR), and caused a reduction in UV survival and cell growth after irradiation. Even though mutation of any of the motifs substantially reduces the accumulation of polη in microscopically visible foci representing replication factories (Bienko et al., 2005), this does not imply that polη is completely excluded from these foci. Rather, the residence time of polη in visible foci could be reduced. This is probably why only a partial reduction in the ability of XP30RO cells reconstituted with any of these mutants to perform TLS past UV-induced damage can be seen. Notably, when combinations of these mutations were tested, UV survival and PRR deficiency was substantially greater. These data show that all these three motifs co-operate to generate a fully functional polη.

We hypothesize that the attachment of Ub to the C-terminus of polη, by inducing an intramolecular interaction with the UBZ, prevents this domain from being engaged in other interactions and also sterically masks the PIR region, hiding it from PCNA. Consistent with this idea, the polη-Ub chimera was deficient in PRR and impaired in rescuing the UV hypersensitivity of XP30RO cells. We anticipate that the natural targeting of Ub to the PIR region would have a similar or even stronger effect than observed in the case of the chimera. We thus propose that the attachment of Ub to the PIR of polη is a mechanism to prevent an unwanted polη–PCNA interaction in undamaged cells (Figure 5C-l). We postulate that the relatively small fraction of monoubiquitinated polη in unperturbed cells represents an equilibrium between ubiquitination and deubiquitination (Figure S5B). Since polη is a very dynamic protein constantly entering replication foci and rapidly leaving them (Sabbioneda et al., 2008), one could envisage that its monoubiquitination (and possibly of other TLS pols) is a process that regulates whether the polymerase stays in or out of replication foci. In the absence of a proper TLS substrate, monoubiquitination would remove it from the focus. Once

back in the nucleoplasm, deubiquitination of polη would restore its TLS-competence and prepare it for new cycles of substrate search.

When the cell is damaged, it is vital that polη and other Y-family polymerases can interact with ubiquitinated PCNA, so that TLS can be carried out at blocked replication forks (Figure 5C-II). Since ubiquitination of polη hinders this interaction, it is of interest that when DNA is damaged by agents known to trigger TLS, ubiquitinated polη is no longer detectable in the cell (Figure 5C-III). Our search for a putative deubiquitinating enzyme (DUB) using two different siRNA libraries, has not to date revealed any candidates (data not shown). Additionally we have not detected any influence of either checkpoint activities or of active nucleotide excision repair on polη ubiquitination or deubiquitination, as they were independent of the presence of either p53, ATR or XPA (Figure S3C-E). Interestingly, we found that HU treatment, which does not damage DNA but prevents fork progression by depleting nucleotide pools, does not result in loss of ubiquitinated polη. Although PCNA is ubiquitinated in HU-treated cells, there should be no requirement for TLS in these cells since there is no DNA damage to be bypassed. It thus appears that deubiquitination of polη occurs only when the polymerase needs to be actually recruited and used. Deubiquitination would ensure that all polη molecules are able to fully interact with ubiquitinated PCNA.

In conclusion, our work provides an interesting example of how the process of monoubiquitination can either positively or negatively regulate the assembly of TLS-competent protein complexes depending on which substrates are modified by ubiquitin. Whereas ubiquitination of PCNA favours its interaction with polη, ubiquitination of polη hinders this interaction, keeping polη away from replication forks.

Experimental procedures

Antibodies and other chemicals

Anti-Flag antibodies were from Sigma (M2 F3165 for WB and M5 F4042 for immunoprecipitation). Anti-polη antibodies used in Figure 1A, Figure 5A and 5B were previously described (Bienko et al., 2005). Elsewhere, anti-polη antibodies were from AbCam (ab17725). Anti-GFP were from BD Biosciences (Living Colours® 632460), anti-p53 from Cell Signalling (#2524), anti-p21 from Santa Cruz (sc-397), anti-phosphoChk1(Ser317) from Cell Signalling (#2344).

Immunoprecipitations and GST pull-downs

Lysates for immunoprecipitations or pull downs were prepared using the "Triton" buffer. Immunoprecipitations and pull-downs were performed lysing a confluent well of a 6-well format plate with 600 μl of the "Triton" buffer, and using 200 μl of lysate plus 200 μl of "Triton" buffer per reaction. After adding the indicated antibodies or GST fusions, the mixture was rotated for 4 h at 4°C. In the case of immunoprecipitations, 15 μl of agarose-Protein A (Medicago) were added per reaction 1 h before the end of rotation. Each sample was then washed 4 times with 600 μl of "Triton" buffer. Agarose or sepharose-beads were resuspended in 25 μl of Laemmli buffer, boiled for 5 min and proteins were separated by SDS-PAGE.

Induction of DNA damage

MRC5 cells were treated and harvested when they were between 50-80% visually confluent. UV (254 nm) treatment was at 0.7 J/m^2/sec in PBS, 30 J/m^2, unless stated otherwise. Recovery was in complete medium for 6 hours (or the time indicated). Cisplatin and transplatin were used for 1 h at 50 μg/ml. Afterwards the medium was changed to allow for recovery. HU and MMS were added directly to the medium for the indicated duration. Cells were either directly scraped into Laemmli buffer and the extract were sonicated before SDS-PAGE, or first collected in a buffer containing benzonase before the addition of Laemmli buffer.

Clonogenic assay

Dilutions of freshly FACS-sorted, XP30RO cell lines expressing wild-type or mutant EGFP-polη from the pEGFP-C3 vector were plated in triplicate on 10 cm dishes in MEM. On the next day the medium was removed and cells were washed in PBS before UV irradiation. After irradiation, cells were incubated in MEM containing 0.4 mM caffeine for 13 days. The number of colonies was assessed after methylene blue staining. Notably, addition of the extra NLS from large T antigen N-terminally to EGFP in the pEGFP constructs did not influence the behaviour of wild-type polη in the assay.

PRR assay

Freshly sorted cells were seeded on 6 cm dishes. After 72 h, the medium was removed, cells washed in PBS and irradiated with 8 J/m^2. Cells were further incubated in 3 ml of medium containing 0.3 mg/ml caffeine for 30 min before the addition of 50 μCi ^{3}H-thymidine. After 30 min, cells were washed in PBS and released in fresh caffeine-containing medium supplemented with 10 μM thymidine and 10 μM deoxycytidine for 150 min. At the end of the chase period, cells were collected in 0.3 ml of PBS containing EDTA (0.2 g/L) and

gamma irradiated (2 krad) to break entangled DNA fibres. Cells were then lysed in 0.2 ml buffer L (2% SDS, 20 mM EDTA) layered on top of 5 ml of a 5-20% sucrose gradient (in 0.1 M NaOH, 0.1 M NaCl). Gradients were spun at 38500 rpm for 90 min in a Sorvall AH650 rotor. At the end of the run, 25 fractions were collected and spotted on Whatman grade 17 paper, precipitated by trichloracetic acid and washed twice in ethanol before being counted on a Beckman scintillation counter (Lehmann et al., 1975). The weight-average molecular weight of the distributions were calculated, omitting the bottom and top three fractions.

Real-time measurement of UV response

XP30RO cells stably transfected with various constructs of pCAG-EGFP-polη were UV irradiated with8 J/m^2 and trypsinized immediately after irradiation. 2500 cells were plated in triplicate in each well of a 96-well E-plate (Roche) in DMEM containing 0.4 mM or 0.8 mM caffeine. Real-time responses of different cell clones to UV were measured using an xCelligence impedentiometer (Roche) according to the manufacturer's instructions (https://www.roche-applied-science.com/sis/xcelligence). The electric impedance through each well was measured every minute over a period of approximately three weeks and recorded as Cell Index (CI).

Details of molecular cloning, production of recombinant proteins, cell culture and sorting, cell lysis, Triton X-100 extraction, mass spectrometry, *in vitro* ubiquitination, laser scanning microscopy, yeast two-hybrid analysis and statistical analysis of the data are presented in Supplemental data.

References

Bennett, E.J., and Harper, J.W. (2008). DNA damage: ubiquitin marks the spot. Nat Struct Mol Biol *15*, 20-22.

Bienko, M., Green, C.M., Crosetto, N., Rudolf, F., Zapart, G., Coull, B., Kannouche, P., Wider, G., Peter, M., Lehmann, A.R.*, et al.* (2005). Ubiquitin-binding domains in Y-family polymerases regulate translesion synthesis. Science *310*, 1821-1824.

Bomar, M.G., Pai, M.T., Tzeng, S.R., Li, S.S., and Zhou, P. (2007). Structure of the ubiquitin-binding zinc finger domain of human DNA Y-polymerase eta. EMBO Rep *8*, 247-251.

Chook, Y.M., and Blobel, G. (2001). Karyopherins and nuclear import. Curr Opin Struct Biol *11*, 703-715.

Finley, D. (2009). Recognition and processing of ubiquitin-protein conjugates by the proteasome. Annu Rev Biochem *78*, 477-513.

Friedberg, E.C., Lehmann, A.R., and Fuchs, R.P. (2005). Trading places: how do DNA polymerases switch during translesion DNA synthesis? Mol Cell *18*, 499-505.

Garg, P., and Burgers, P.M. (2005). Ubiquitinated proliferating cell nuclear antigen activates translesion DNA polymerases eta and REV1. Proc Natl Acad Sci U S A *102*, 18361-18366.
Gueranger, Q., Stary, A., Aoufouchi, S., Faili, A., Sarasin, A., Reynaud, C.A., and Weill, J.C. (2008). Role of DNA polymerases eta, iota and zeta in UV resistance and UV-induced mutagenesis in a human cell line. DNA Repair (Amst) *7*, 1551-1562.
Gulbis, J.M., Kelman, Z., Hurwitz, J., O'Donnell, M., and Kuriyan, J. (1996). Structure of the C-terminal region of p21(WAF1/CIP1) complexed with human PCNA. Cell *87*, 297-306.
Guo, C., Fischhaber, P.L., Luk-Paszyc, M.J., Masuda, Y., Zhou, J., Kamiya, K., Kisker, C., and Friedberg, E.C. (2003). Mouse Rev1 protein interacts with multiple DNA polymerases involved in translesion DNA synthesis. EMBO J *22*, 6621-6630.
Guo, C., Tang, T.S., Bienko, M., Dikic, I., and Friedberg, E.C. (2008). Requirements for the interaction of mouse Polkappa with ubiquitin and its biological significance. J Biol Chem *283*, 4658-4664.
Guo, C., Tang, T.S., Bienko, M., Parker, J.L., Bielen, A.B., Sonoda, E., Takeda, S., Ulrich, H.D., Dikic, I., and Friedberg, E.C. (2006). Ubiquitin-binding motifs in REV1 protein are required for its role in the tolerance of DNA damage. Mol Cell Biol *26*, 8892-8900.
Haglund, K., and Dikic, I. (2005). Ubiquitylation and cell signaling. EMBO J *24*, 3353-3359.
Haracska, L., Johnson, R.E., Unk, I., Phillips, B., Hurwitz, J., Prakash, L., and Prakash, S. (2001). Physical and functional interactions of human DNA polymerase eta with PCNA. Mol Cell Biol *21*, 7199-7206.
Hicke, L. (2001). Protein regulation by monoubiquitin. Nat Rev Mol Cell Biol *2*, 195-201.
Hishiki, A., Hashimoto, H., Hanafusa, T., Kamei, K., Ohashi, E., Shimizu, T., Ohmori, H., and Sato, M. (2009). Structural Basis for Novel Interactions between Human Translesion Synthesis Polymerases and Proliferating Cell Nuclear Antigen. J Biol Chem *284*, 10552-10560.
Hoege, C., Pfander, B., Moldovan, G.L., Pyrowolakis, G., and Jentsch, S. (2002). RAD6-dependent DNA repair is linked to modification of PCNA by ubiquitin and SUMO. Nature *419*, 135-141.
Hoeller, D., Crosetto, N., Blagoev, B., Raiborg, C., Tikkanen, R., Wagner, S., Kowanetz, K., Breitling, R., Mann, M., Stenmark, H., and Dikic, I. (2006). Regulation of ubiquitin-binding proteins by monoubiquitination. Nat Cell Biol *8*, 163-169.
Hoeller, D., Hecker, C.M., Wagner, S., Rogov, V., Dotsch, V., and Dikic, I. (2007). E3-independent monoubiquitination of ubiquitin-binding proteins. Mol Cell *26*, 891-898.
Hurley, J.H., Lee, S., and Prag, G. (2006). Ubiquitin-binding domains. Biochem J *399*, 361-372.
Johnson, R.E., Kondratick, C.M., Prakash, S., and Prakash, L. (1999). hRAD30 mutations in the variant form of xeroderma pigmentosum. Science *285*, 263-265.
Kannouche, P., Broughton, B.C., Volker, M., Hanaoka, F., Mullenders, L.H., and Lehmann, A.R. (2001). Domain structure, localization, and function of DNA polymerase eta, defective in xeroderma pigmentosum variant cells. Genes Dev *15*, 158-172.
Kannouche, P., Fernandez de Henestrosa, A.R., Coull, B., Vidal, A.E., Gray, C., Zicha, D., Woodgate, R., and Lehmann, A.R. (2003). Localization of DNA polymerases eta and iota to the replication machinery is tightly co-ordinated in human cells. EMBO J *22*, 1223-1233.
Kannouche, P.L., and Lehmann, A.R. (2004). Ubiquitination of PCNA and the polymerase switch in human cells. Cell Cycle *3*, 1011-1013.
Kannouche, P.L., Wing, J., and Lehmann, A.R. (2004). Interaction of human DNA polymerase eta with monoubiquitinated PCNA: a possible mechanism for the polymerase switch in response to DNA damage. Mol Cell *14*, 491-500.
Kirkin, V., McEwan, D.G., Novak, I., and Dikic, I. (2009). A role for ubiquitin in selective autophagy. Mol Cell *34*, 259-269.

Koken, M.H., Reynolds, P., Jaspers-Dekker, I., Prakash, L., Prakash, S., Bootsma, D., and Hoeijmakers, J.H. (1991). Structural and functional conservation of two human homologs of the yeast DNA repair gene RAD6. Proc Natl Acad Sci U S A *88*, 8865-8869.
Lehmann, A.R., Kirk-Bell, S., Arlett, C.F., Paterson, M.C., Lohman, P.H., de Weerd-Kastelein, E.A., and Bootsma, D. (1975). Xeroderma pigmentosum cells with normal levels of excision repair have a defect in DNA synthesis after UV-irradiation. Proc Natl Acad Sci U S A *72*, 219-223.
Maga, G., and Hubscher, U. (2003). Proliferating cell nuclear antigen (PCNA): a dancer with many partners. J Cell Sci *116*, 3051-3060.
Masutani, C., Araki, M., Yamada, A., Kusumoto, R., Nogimori, T., Maekawa, T., Iwai, S., and Hanaoka, F. (1999). Xeroderma pigmentosum variant (XP-V) correcting protein from HeLa cells has a thymine dimer bypass DNA polymerase activity. EMBO J *18*, 3491-3501.
McCulloch, S.D., Kokoska, R.J., Masutani, C., Iwai, S., Hanaoka, F., and Kunkel, T.A. (2004). Preferential cis-syn thymine dimer bypass by DNA polymerase eta occurs with biased fidelity. Nature *428*, 97-100.
Mukhopadhyay, D., and Riezman, H. (2007). Proteasome-independent functions of ubiquitin in endocytosis and signaling. Science *315*, 201-205.
Ogi, T., Kannouche, P., and Lehmann, A.R. (2005). Localisation of human Y-family DNA polymerase kappa: relationship to PCNA foci. J Cell Sci *118*, 129-136.
Plosky, B.S., Vidal, A.E., Fernandez de Henestrosa, A.R., McLenigan, M.P., McDonald, J.P., Mead, S., and Woodgate, R. (2006). Controlling the subcellular localization of DNA polymerases iota and eta via interactions with ubiquitin. EMBO J *25*, 2847-2855.
Sabbioneda, S., Gourdin, A.M., Green, C.M., Zotter, A., Giglia-Mari, G., Houtsmuller, A., Vermeulen, W., and Lehmann, A.R. (2008). Effect of proliferating cell nuclear antigen ubiquitination and chromatin structure on the dynamic properties of the Y-family DNA polymerases. Mol Biol Cell *19*, 5193-5202.
Sabbioneda, S., Green, C.M., Bienko, M., Kannouche, P., Dikic, I., and Lehmann, A.R. (2009). Ubiquitin-binding motif of human DNA polymerase eta is required for correct localization. Proc Natl Acad Sci U S A *106*, E20; author reply E21.
Sakurai, S., Kitano, K., Yamaguchi, H., Hamada, K., Okada, K., Fukuda, K., Uchida, M., Ohtsuka, E., Morioka, H., and Hakoshima, T. (2005). Structural basis for recruitment of human flap endonuclease 1 to PCNA. EMBO J *24*, 683-693.
Tateishi, S., Sakuraba, Y., Masuyama, S., Inoue, H., and Yamaizumi, M. (2000). Dysfunction of human Rad18 results in defective postreplication repair and hypersensitivity to multiple mutagens. Proc Natl Acad Sci U S A *97*, 7927-7932.
Watanabe, K., Tateishi, S., Kawasuji, M., Tsurimoto, T., Inoue, H., and Yamaizumi, M. (2004). Rad18 guides poleta to replication stalling sites through physical interaction and PCNA monoubiquitination. EMBO J *23*, 3886-3896.
Woelk, T., Oldrini, B., Maspero, E., Confalonieri, S., Cavallaro, E., Di Fiore, P.P., and Polo, S. (2006). Molecular mechanisms of coupled monoubiquitination. Nat Cell Biol *8*, 1246-1254.
Yang, W., and Woodgate, R. (2007). What a difference a decade makes: insights into translesion DNA synthesis. Proc Natl Acad Sci U S A *104*, 15591-15598.

Acknowledgments

We thank Blagoy Blagoev for initial mass spectrometry experiments. We are grateful to Zvi Livneh, Ayal Hendel, Patricia Kannouche, Titia Sixma, Tirzah Braz Petta and Tina Perica for

advice and help on this project. This work was supported by grants from Deutsche Forschungsgemeinschaft, the Cluster of Excellence "Macromolecular Complexes" of the Goethe University Frankfurt (EXC115) (to I.D.); from ESF Eurodyna program, the UK Medical Research Council, and an EU integrated project on DNA Repair (to A.R.L.) and by the Josef Buchmann Scholarship (to M.B.).

Figure legends

Figure 1 – Monoubiquitination sites lie in the C-terminal portion of polη. A) Anti-polη immunoblot of lysates of MRC5 and XP30RO cells. B) HEK293T cells were transfected with various Flag-polη constructs and lysates were analyzed by anti-Flag (M2) immunoblot after immunoprecipitation with anti-Flag (M5) antibodies. C) Amino acid sequence of the C-terminus of polη from human, mouse and frog. Cysteines and histidines of UBZ and conserved lysines around NLS are highlighted. D) Scheme of various constructs of polη. Lower panel shows the C-terminus of the constructs (as marked by the dashed rectangle in the upper panel) depicting the position of amino acids mutated. CD: catalytic domain, UBZ: ubiquitin-binding zinc-finger, N: NLS, P: PIP box, N*: NLS of the SV40 large T antigen. E) MRC5 cells transiently expressing indicated EGFP-tagged polη variants were analysed by confocal microscopy. Representative midplane sections are shown together with DAPI images in blue. See also Figure S1.

Figure 2 – Identification of PIR as a PCNA-interaction surface. A) One-on-one interaction assay using yeast two-hybrid system. The upper panel shows equal growth of all yeast used for testing polη-PCNA interaction. The same plate was used for the β-x-gal test (middle panel). The lower panel shows growth on a selection medium to probe for interaction between bait and prey proteins. EV: empty pYTH9 or pACT2. B) GST pull-down of PCNA by various mutants of the C-terminus of polη. C) GST pull-down with a range of purified PCNA concentrations using GST, GST-polηWT, GST-polηNLS* or GST-polηPIP*. D) HEK293T cells were transfected with various pEGFP-polη constructs and their lysates were used in GST-PCNA pull-down. Means and SD of three independent experiments are shown in the histogram. See also Figure S2.

Figure 3 – Influence of polη-PCNA interaction on localization of polη into replication foci and on TLS. A) MRC5 cells transfected with various pEGFP-polη constructs were analysed

by confocal microscopy. B) Quantification of data presented in A. The histogram represents means and SD calculated after counting 300 cells in each of three independent experiments with each construct. “NLS-WT” and “WT” differ by the presence of an extra copy of the NLS from the SV40 large T antigen in the former one, as depicted in Figure 1D. C) Clonogenic survival assay with XP30RO-derived cell lines expressing the indicated EGFP-polη constructs after UV irradiation with different doses and growth in 0.4 mM caffeine-containing medium (UBZ*: polηD652A; EV: empty vector). Error bars: SD from three independent experiments. D) Alkaline sucrose sedimentation analysis of DNA from cells pulsed for 30 min with ^{3}H-thymidine and chased for 150 min after 8 J/m^2 UV irradiation (PRR assay). Polη single or double mutants were compared to one cell line proficient in damage bypass (XP30RO complemented with wt polη) and one defective (XP30RO with empty vector) in the same experiment. The relative average molecular weights of the distributions are presented in the histograms after normalization to that of the wild-type polη-complemented cells. Means and SD from three independent experiments are shown. E) Real-time monitoring of UV-response of XP30RO cell lines grown in 0.4 mM caffeine-containing medium after UV-irradiation with 8 J/m^2. Dashed color-matched lines show the SD of the results from three separate wells treated in the same manner. Left inset: semi-logarithmic plot of the decay phase. Right inset: re-growth phase of WT, NLS* and PIP*; dashed grey lines: fitted Boltzmann’s sigmoid curves. See also Figure S3.

Figure 4 – Effects of monoubiquitination of the C-terminus of polη on its localization, PCNA-interaction and TLS. A) Schematic representation of polη-Ub chimera including only the C-terminal part of polη shown in the intramolecular-bound state. B) MRC5 cells transfected with various pEGFP-polη constructs were analysed by confocal microscopy as in Figure 3A. C) Quantification of data presented in B as in figure 3B. D) XP30RO cells stably expressing EGFP-polη or an empty vector were extracted by Triton X-100 by method A (see Supplemental data) and the ubiquitination of polη was compared in total cell extracts (TCL), triton-soluble (TS) and triton-resistant fractions (TRF). E) GST-PCNA pull-down using lysates of HEK293T cells transfected with either pEGFP-polη or pEGFP-polη-Ub. Means and SD of three independent experiments are shown in the histogram. F) Clonogenic survival assay of XP30RO-derived cell lines expressing the indicated EGFP-polη constructs (EV: empty vector). Error bars represent the SD from three independent experiments. G) PRR assay with the pEGFP-polη-Ub cell line in comparison to polη wild-type or empty vector

(EV) lines. The relative average molecular weights of the distributions are presented in the histogram after normalization to that of the wild-type polη-complemented cells. Error bars represent the SD from three independent experiments. See also Figure S4.

Figure 5 – Monobiquitination of polη is down-regulated after DNA damage. Endogenous polη in MRC5 cells treated with either UV (A), cisplatin, transplatin, methyl methane sulfonate (MMS) or hydroxyurea (HU) (B) as indicated. C) Model for effect of ubiquitination on interaction between PCNA and polη. UBZ-mediated monoubiquitination of polη can result in intramolecular interaction between Ub and the UBZ, in turn keeping polη away from PCNA engaged in replication. Following UV irradiation, monoubiquitination of PCNA and deubiquitination of polη facilitate interaction between the two proteins. For simplicity, only polη C-terminus is shown.

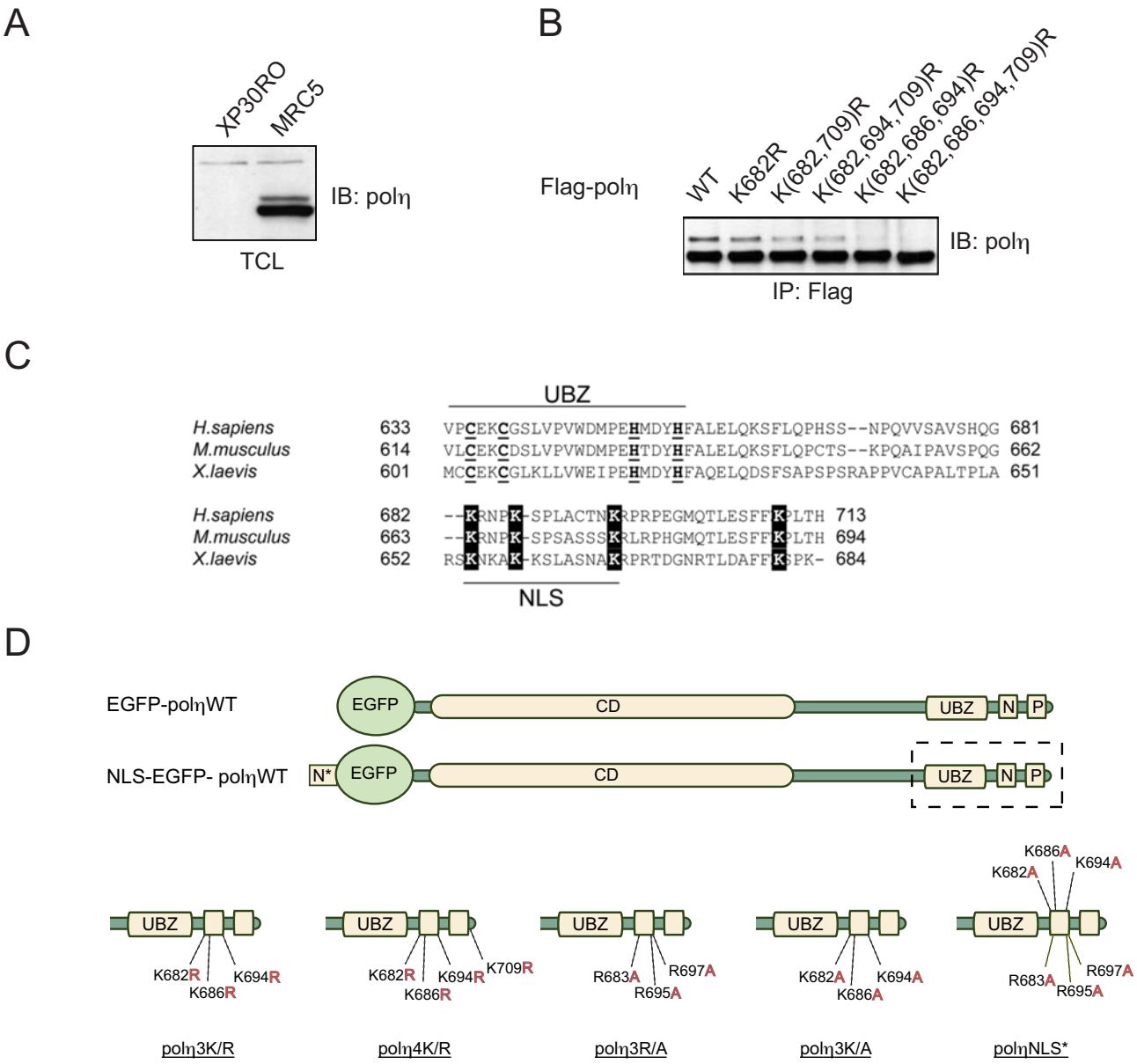
A
XP30RO
MRC5
IB: polη
TCL
B
Flag-polη
WT
K682R
K(682,709)R
K(682,694,709)R
K(682,686,694)R
K(682,686,694,709)R
IB: polη
IP: Flag
C
UBZ
H.sapiens 633 VPCEKCGSLVPVWDMPEHMDYHFALELQKSFLQPHSS--NPQVVSAVSHQG 681
M.musculus 614 VLCEKCDSLVPVWDMPEHTDYHFALELQKSFLQPCTS--KPQAIPAVSPQG 662
X.laevis 601 MCCEKCGLKLLVWEIPEHMDYHFAQELQDSFSAPSPSRAPPVCAPALTPLA 651
H.sapiens 682 --KRNPK-SPLACTNKRPRPEGMQTLESFFKPLTH 713
M.musculus 663 --KRNPK-SPSASSSKRLRPHGMQTLESFFKPLTH 694
X.laevis 652 RSKNKAK-KSLASNAKRPRTDGNRTLDAFFKSPK- 684
NLS
D
EGFP-polηWT
EGFP
CD
UBZ
N
P
NLS-EGFP- polηWT
N*
K682R
K686R
K694R
K709R
R683A
R695A
R697A
K682A
K686A
K694A
polη3K/R
polη4K/R
polη3R/A
polη3K/A
polηNLS*
E
EGFP-polηWT
Merge
NLS-EGFP-polηWT
EGFP-polη4K/R
NLS-EGFP-polη4K/R
10 μm

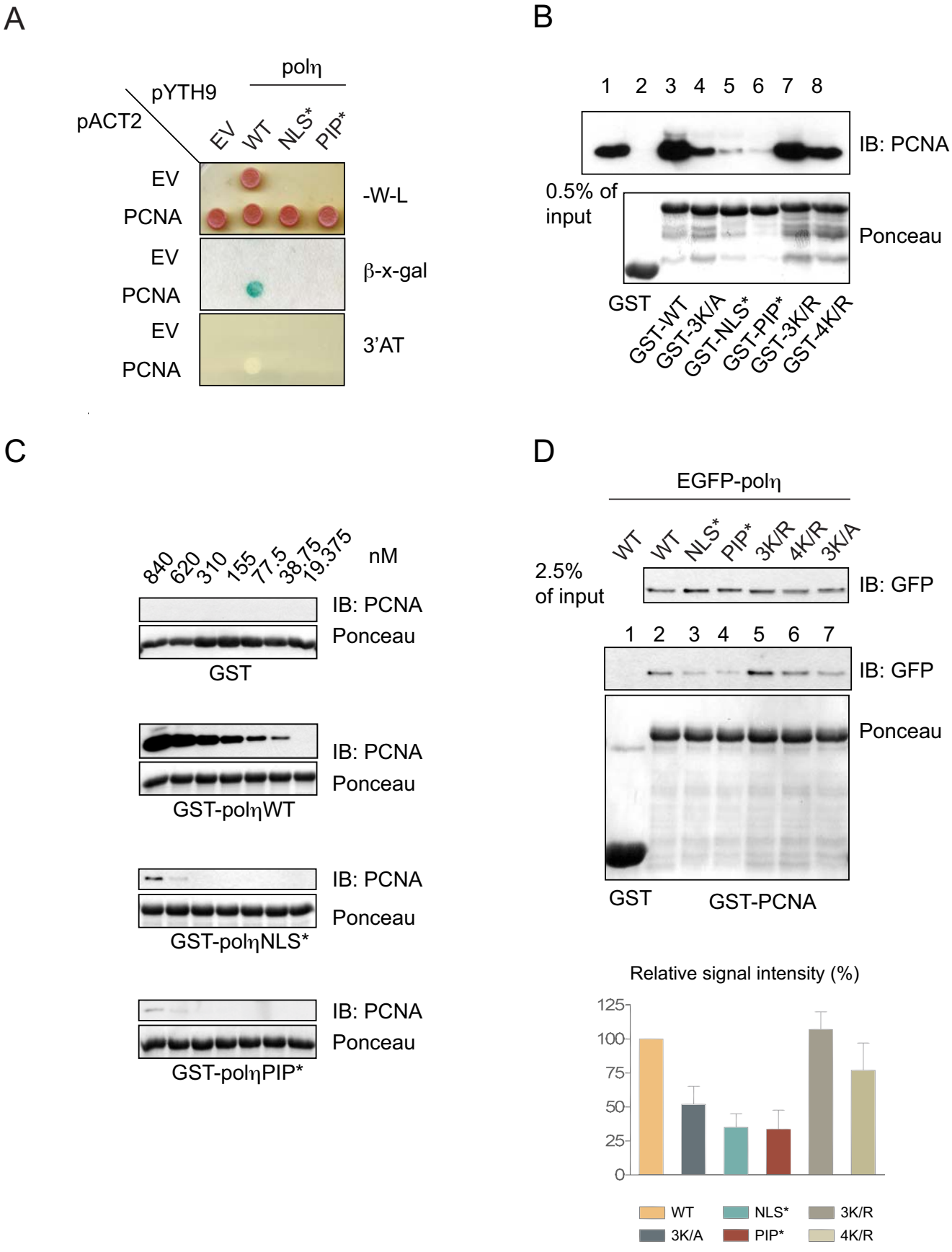
A
polη
pYTH9
pACT2
EV
WT
NLS*
PIP*
EV
PCNA
-W-L
β-x-gal
3'AT
B
1 2 3 4 5 6 7 8
IB: PCNA
0.5% of input
Ponceau
GST
GST-WT
GST-3K/A
GST-NLS*
GST-PIP*
GST-3K/R
GST-4K/R
C
840 620 310 155 77.5 38.75 19.375 nM
IB: PCNA
Ponceau
GST
GST-polηWT
GST-polηNLS*
GST-polηPIP*
D
EGFP-polη
WT WT NLS* PIP* 3K/R 4K/R 3K/A
2.5% of input
IB: GFP
1 2 3 4 5 6 7
Ponceau
GST
GST-PCNA
Relative signal intensity (%)
125
100
75
50
25
0
WT
NLS*
3K/R
3K/A
PIP*
4K/R

Figure 3

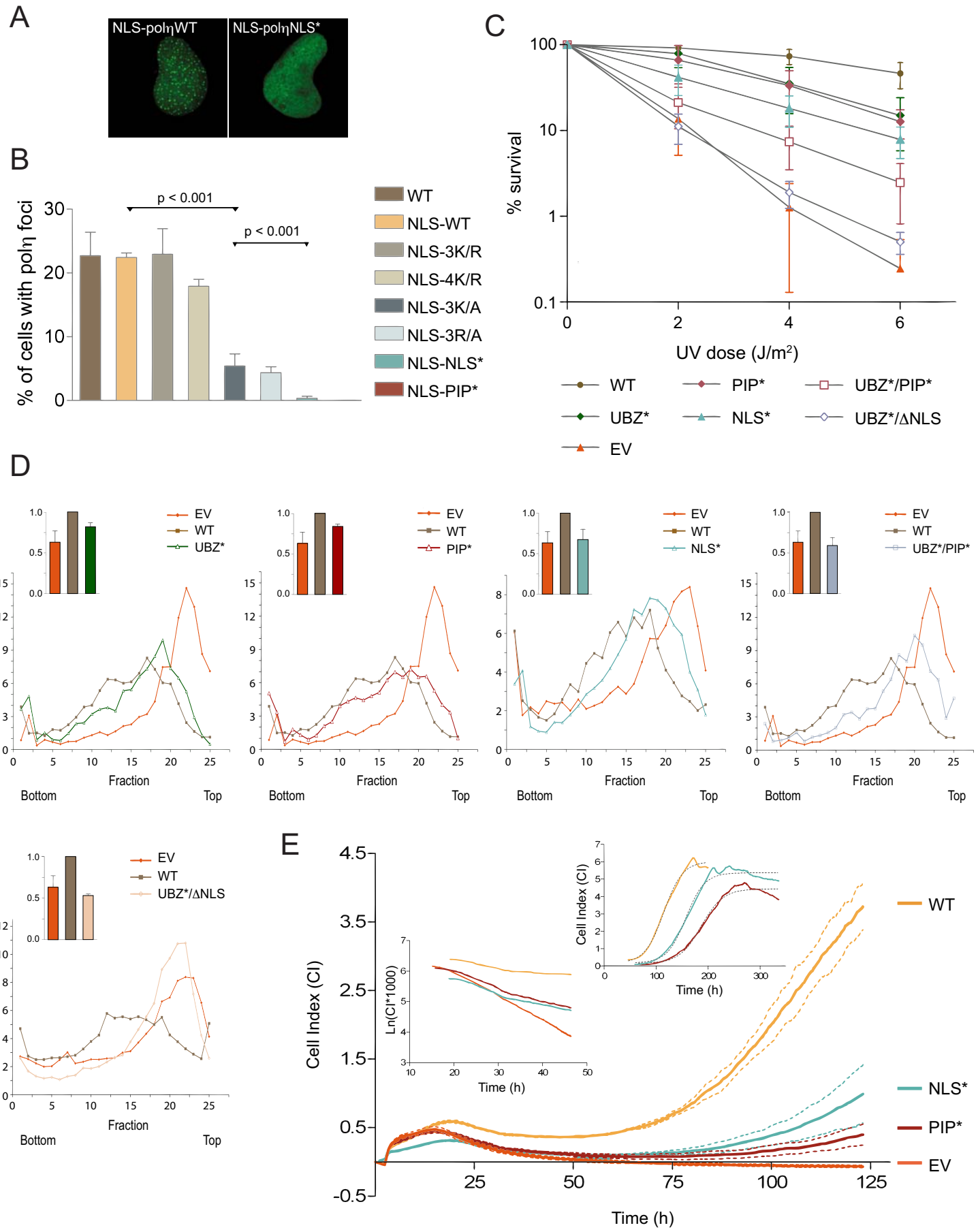
A
NLS-polηWT
NLS-polηNLS*
B
% of cells with polη foci
p < 0.001
p < 0.001
WT
NLS-WT
NLS-3K/R
NLS-4K/R
NLS-3K/A
NLS-3R/A
NLS-NLS*
NLS-PIP*
C
% survival
UV dose (J/m²)
WT
UBZ*
EV
PIP*
NLS*
UBZ*/PIP*
UBZ*/ΔNLS
D
% of total cpm
Fraction
Bottom
Top
EV
WT
UBZ*
PIP*
NLS*
UBZ*/PIP*
UBZ*/ΔNLS
E
Cell Index (CI)
Time (h)
Ln(CI*1000)
WT
NLS*
PIP*
EV

Figure 4

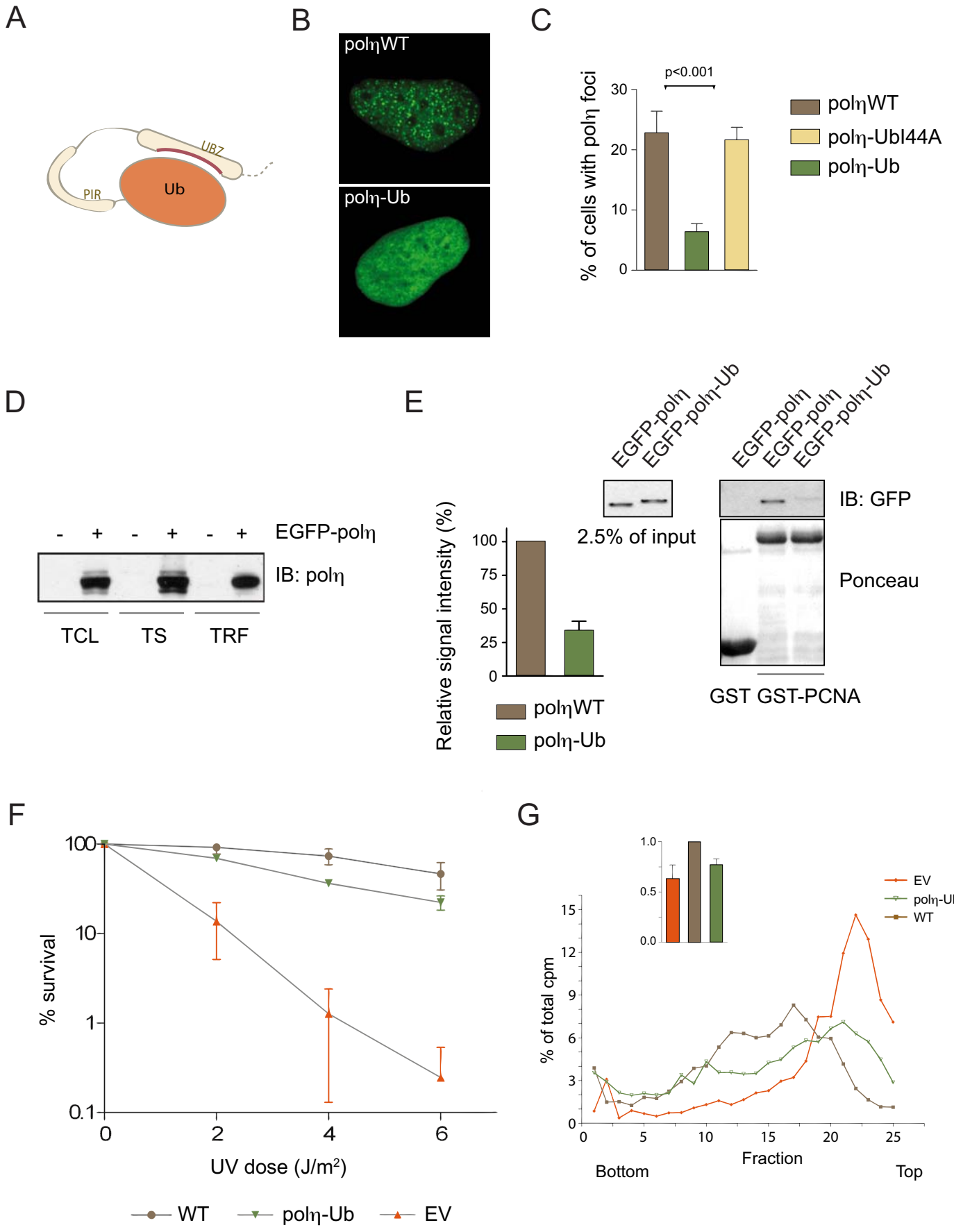
A
UBZ
PIR
Ub
B
polηWT
polη-Ub
C
p<0.001
% of cells with polη foci
30
20
10
0
polηWT
polη-UbI44A
polη-Ub
D
- + - + - +
EGFP-polη
IB: polη
TCL
TS
TRF
E
EGFP-polη
EGFP-polη-Ub
EGFP-polη
EGFP-polη
EGFP-polη-Ub
IB: GFP
2.5% of input
Ponceau
Relative signal intensity (%)
100
75
50
25
0
polηWT
polη-Ub
GST GST-PCNA
F
100
10
1
0.1
% survival
0
2
4
6
UV dose (J/m²)
WT
polη-Ub
EV
G
1.0
0.5
0.0
15
12
9
6
3
0
% of total cpm
0
5
10
15
20
25
Fraction
Bottom
Top
EV
polη-Ub
WT

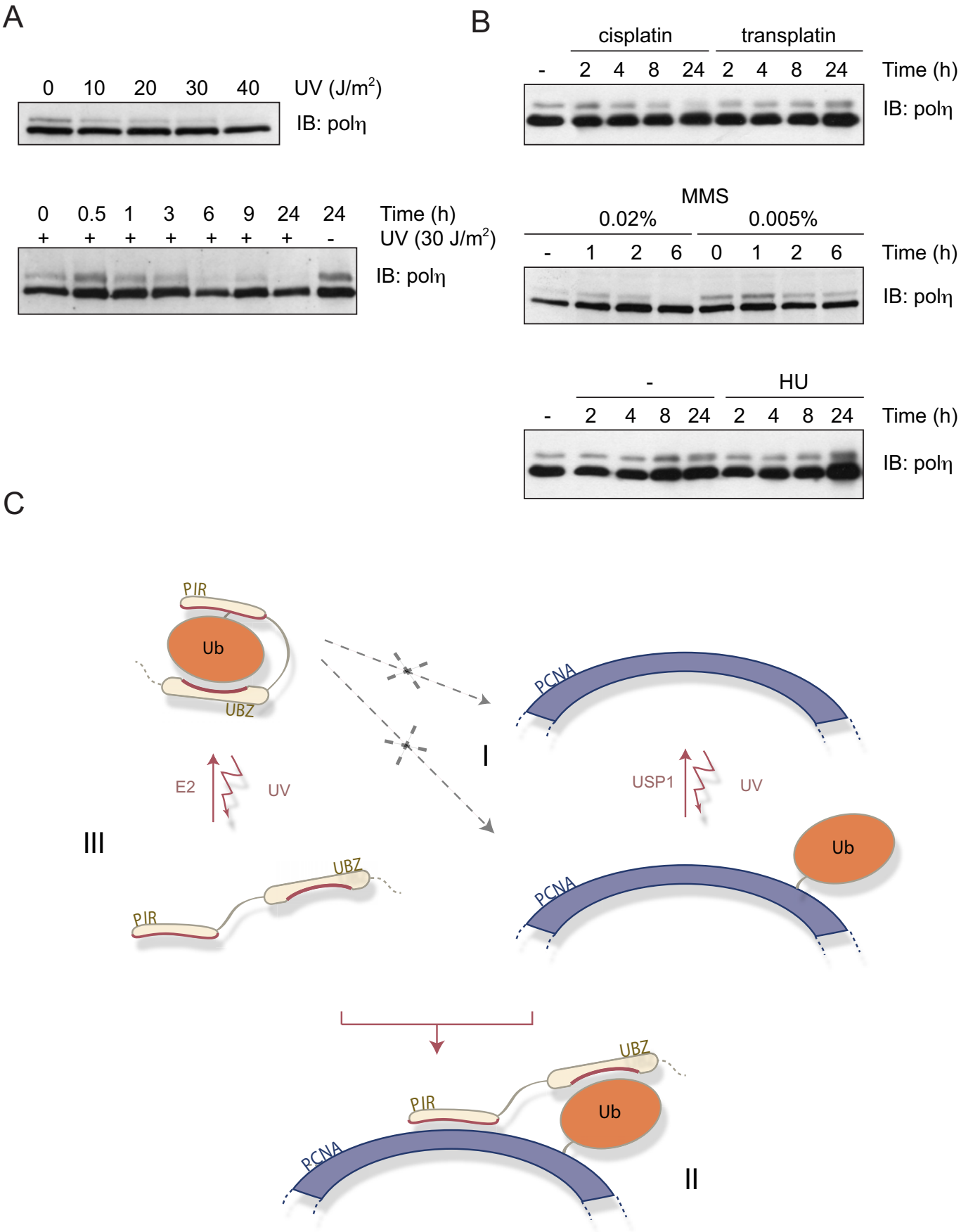
A
0 10 20 30 40
UV (J/m2)
IB: polη
0 0.5 1 3 6 9 24 24
+ + + + + + + -
Time (h)
UV (30 J/m2)
IB: polη
B
cisplatin
transplatin
- 2 4 8 24 2 4 8 24
Time (h)
IB: polη
MMS
0.02%
0.005%
- 1 2 6 0 1 2 6
Time (h)
IB: polη
-
HU
- 2 4 8 24 2 4 8 24
Time (h)
IB: polη
C
PIR
Ub
UBZ
E2
UV
III
I
PCNA
USP1
UV
Ub
PCNA
UBZ
PIR
UBZ
PIR
Ub
PCNA
II

Inventory of Supplemental Information

- ✓ Supplemental Data:
  - Figure S1, related to Figure 1
  - Figure S2, related to Figure 2
  - Figure S3, related to Figure 3
  - Figure S4, related to Figure 4
  - Figure S5, related to Discussion section
  - Table S1, related to Figure 2
  - Table S2, related to Figure 3
  - Table S3, related to Figure 3
- ✓ Supplemental Experimental Procedures
- ✓ Supplemental References

Supplemental Data

Figure S1

Bienko *et al.*

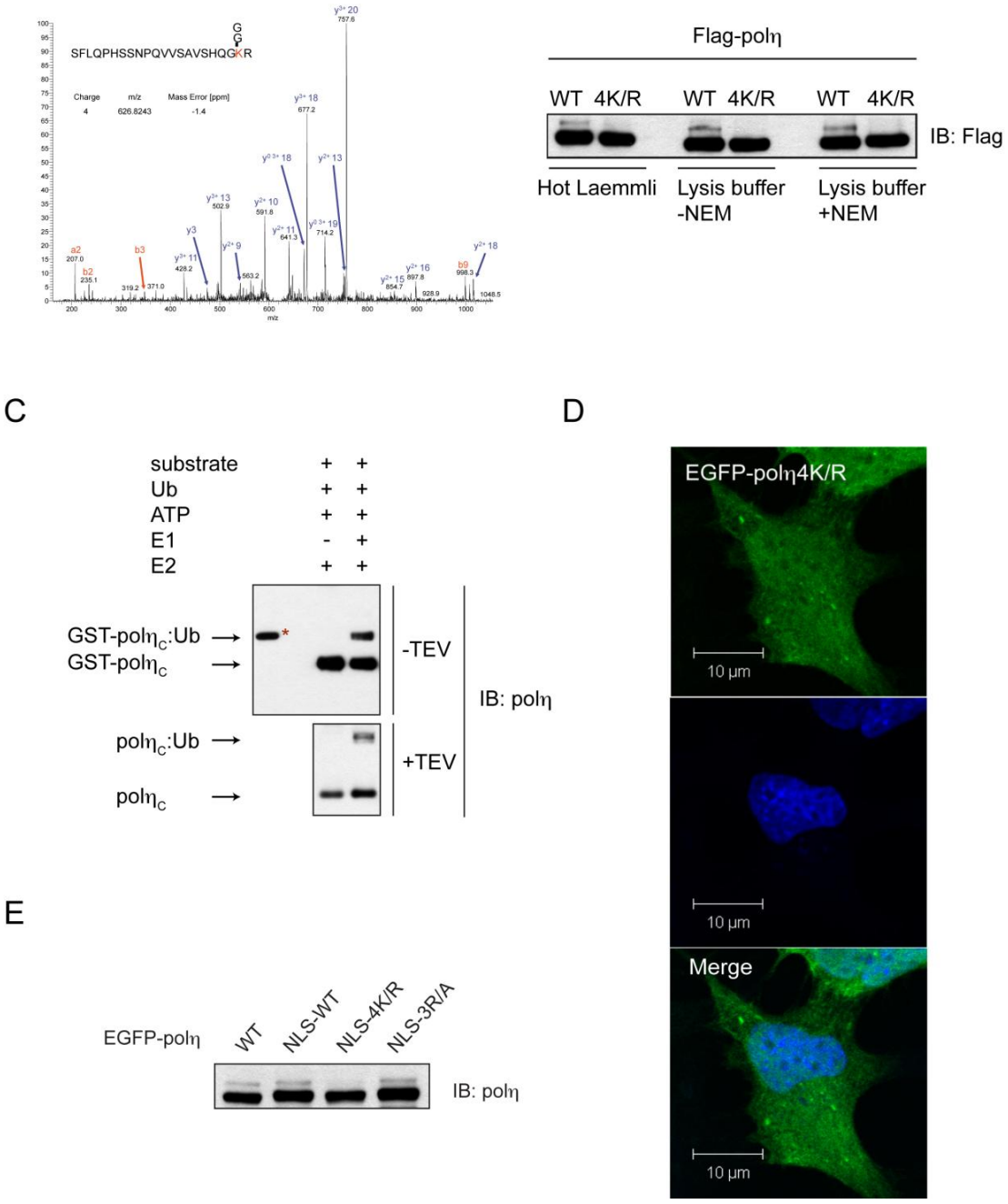

Figure S1. A) Mapping of ubiquitination sites by mass spectrometry is based on the detection of a +114 Da increase in the mass of the modified lysine after tryptic digestion. This mass shift is due to the presence of two glycines derived from the C-terminus of ubiquitin attached to the target lysine. The figure shows the MS/MS fragmentation spectrum of the ubiquitinated K682-containing peptide. Precursor ion mass was measured in the FT-ICR analyzer. After fragmentation of the peptide by collision-induced fragmentation, the masses of the fragment ions were acquired in the linear ion trap. B) HEK293T transfected with Flag-polη WT or 4K/R were lysed using three different lysis conditions. Lysis buffer stands for "Triton" buffer. C) *In vitro* ubiquitination of the C-terminal fragment of polη. GST-fused amino acids 602-713 of polη (GST-polη_C) were incubated with the ubiquitination mix either in the absence or presence of Ub-activating enzyme (E1). Unmodified and ubiquitinated products were detected by polη immunoblot before and after cleaving the GST tag off by TEV protease. Red asterisk: a genetic GST-Ub-polη_C fusion used as size reference for *in vitro* ubiquitinated GST-polη_C. E2: Ub-conjugating enzyme. D) MRC5 cells transiently expressing EGFP-polη4KRwere analysed by confocal microscopy. Representative mid-plane section of a non-S phase cell is shown together with DAPI stain in blue. E) Extracts of HEK293T cells transfected with different pEGFP-polη constructs were analyzed by immunoblot with anti-polη antibodies after lysis with hot Laemmli buffer.

Figure S2

Bienko *et al.*

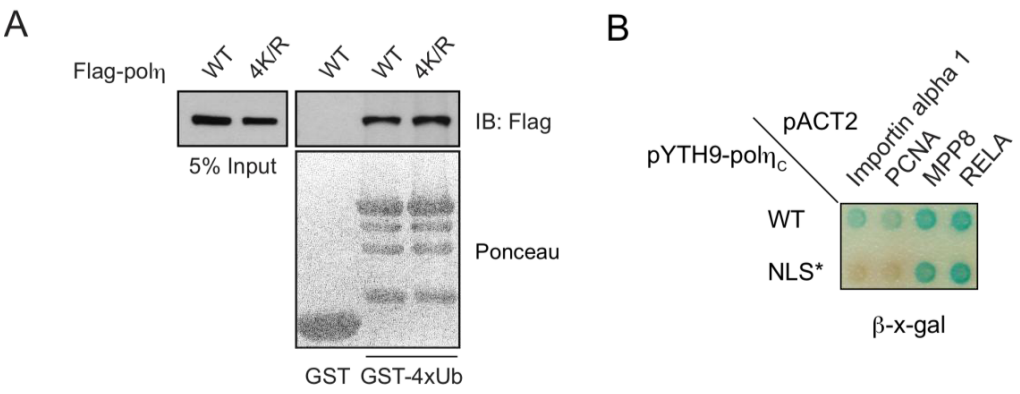

Figure S2. A) GST-4xUb pull down using lysates of HEK293T cells transfected with either Flag-polη or Flag-polη4K/R. B) Yeast two-hybrid assay of clones found in the library screen with wild-type polη$_C$, testing their ability to interact with its NLS mutant.

Figure S3

Bienko *et al.*

A

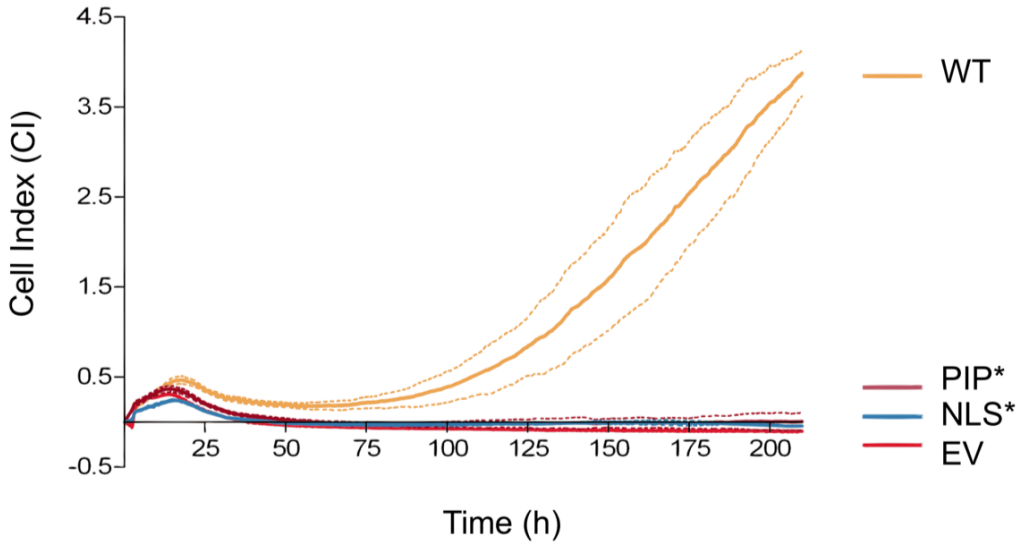

B

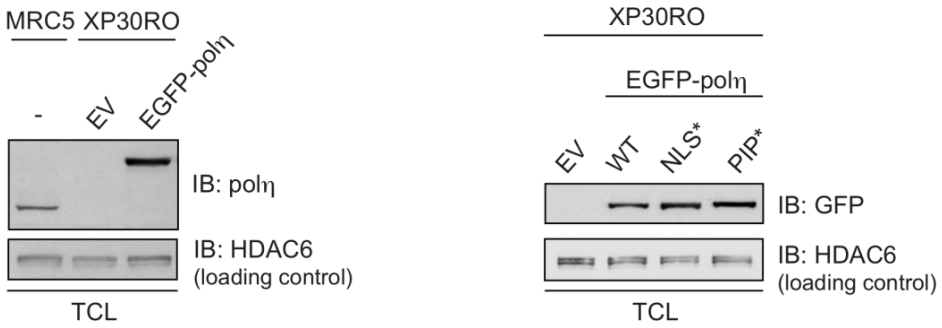

Figure S3. A) Real-time monitoring of UV response of XP30RO cell lines grown in 0.8 mM caffeine-containing medium after UV irradiation with 8 J/m^2. Dashed color-matched lines show the SD of the results from three separate wells treated in the same manner. B) Expression levels of pCAG constructs in XP30RO-derived cell lines. Left: comparison with endogenous polη in MRC5. Right: comparison between different pCAG constructs-expressing cell lines (EV: empty vector).

Figure S4

Bienko *et al.*

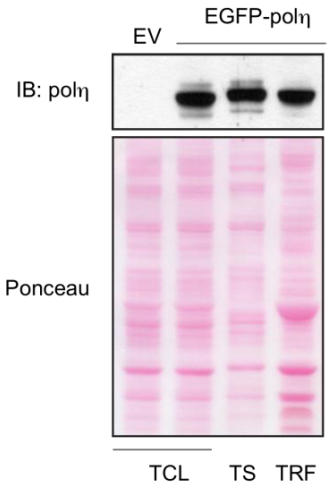

Figure S4. XP30RO cells stably expressing EGFP-polη or an empty vector were extracted by Triton X-100 using method B (see Supplemental data) and the ubiquitination of polη was compared in total cell extracts (TCL), triton-soluble (TS) and triton-resistant fractions (TRF).

Figure S5

Bienko *et al.*

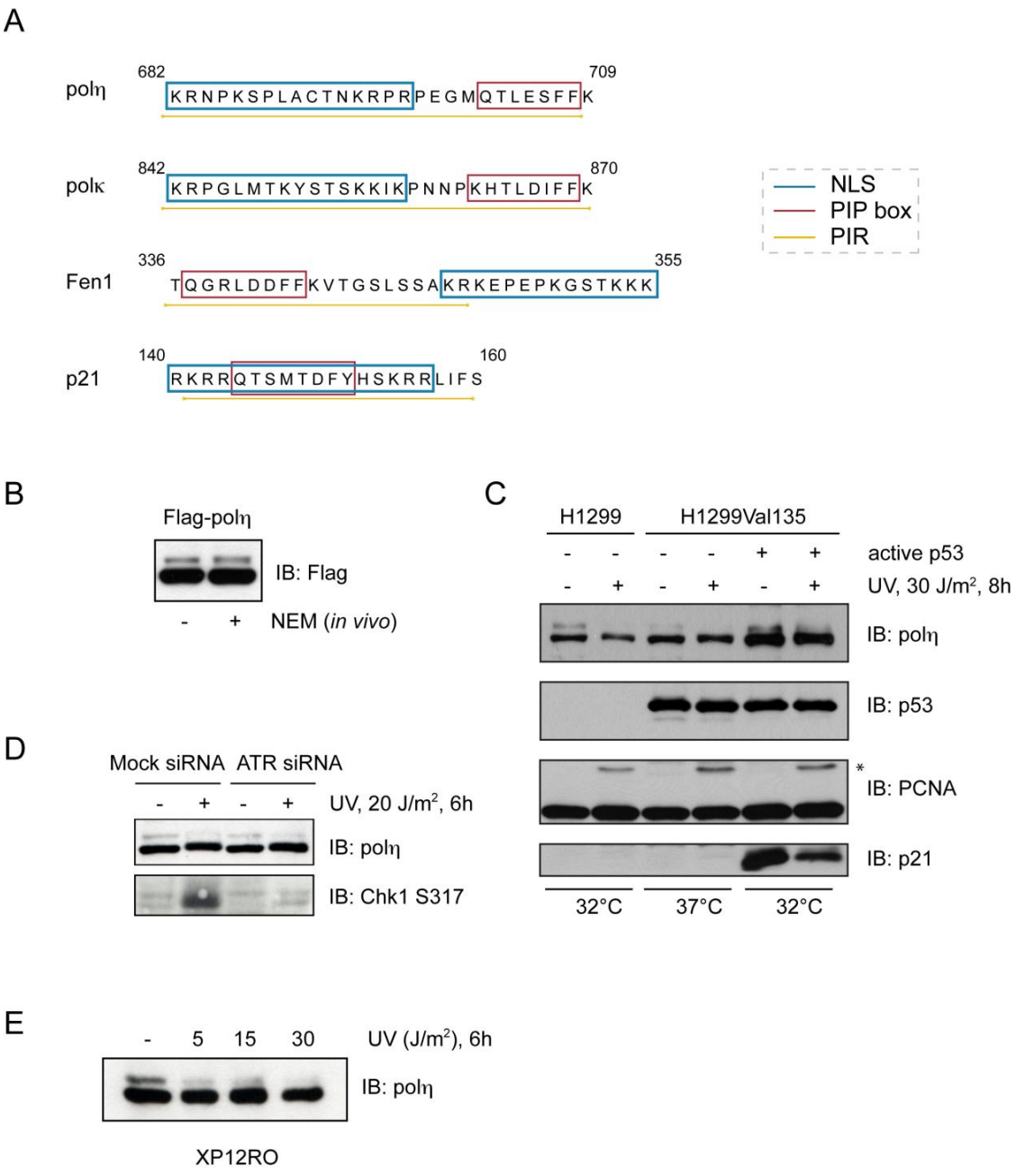

Figure S5. A) Primary sequence of PIP box motifs (in red) in polη, polκ, Fen1 and p21 showing their position in respect to the NLS (in blue). In yellow: the PCNA-Interacting Region (PIR), including PIP box and additional regions shown to interact with PCNA either in this manuscript (polη and polκ) or by others (Gulbis et al., 1996; Hishiki et al., 2009; Sakurai et al., 2005). Numbers indicate the first and last amino acid of the regions shown. B) HEK293T were transfected with Flag-polη. 45 min before lysis in hot Laemmli buffer, NEM was added to the medium to a final 10 mM concentration. C) H1299 p53-negative cells and H1299Val135 cells, expressing a temperature-sensitive mutant of p53 active at 32°C, were UV irradiated and tested for the presence or absence of UV-induced deubiquitination of polη. The PCNA immunoblot indicates a similar response of all cells to UV by the appearance of monoubiquitinated PCNA (indicated by *), while the p21 immunoblot proves the activity of p53 in H1299Val135 cells grown at 32°C. All cells were lysed with hot Laemmli buffer. D) MRC5 cells were transfected with a control siRNA (mock) or siRNA against ATR. Two days after transfection cells were UV irradiated and after 6 h further incubation they were lysed using Laemmli buffer followed by immunoblot. E) XP12RO cells, deficient in XPA and unable to conduct NER, were UV irradiated with the indicated doses and lysed in Laemmli buffer 6 h after irradiation.

Table S1. List of clones found in the yeast two-hybrid screen with the C-terminal fragment of polη as bait.

Name	Accession number	# of clones
Importin alpha 1 (KPNA2)	NP_002257	2
Proliferating Cell Nuclear Antigen (PCNA)	NP_002583	2
M-phase phosphoprotein 8 (MPP8)	NP_059990	2
V-rel reticuloendotheliosis viral oncogene homolog A (RELA)	NP_068810	3
Mediator complex subunit 10 (NUT2)	NP_115662	2
Nucleophosmin 1 (NMP1)	NP_002511	1
Hypothetical protein LOC54914	NP_060264	1
Eukaryotic translation initiation factor 3, subunit 6 (EIF3-P48)	NP_001559	1

Table S2. In blue: fitted parameters after linear regression of clonogenic assay results. In red: results of F test applied to clonogenic assay data after linear regression.

	D_{50} (J/m^2)	SLOPE	R^2
EV	0,67	-1,0270	0,9954
WT	6,45	-0,1074	0,8658
polη-Ub	2,82	-0,2460	0,9871
PIP*	2,21	-0,3141	0,9563
NLS*	1,63	-0,4256	0,9999
UBZ*	2,42	-0,2861	0,9290
COMPARISONS BETWEEN PAIRS			
	P (F test)	**F(DFn;DFd)**	
WT vs EV	0,0001	989,8 (1;6)	
WT vs PIP*	0,0005	46,38 (1;6)	
WT vs NLS*	0,0001	351,5 (1;6)	
WT vs polη-Ub	0,0004	49,61 (1;6)	
WT vs UBZ*	0,0022	26,07 (1;6)	
PIP* vs polη-Ub	0,0463	6,271 (1;6)	
PIP* vs UBZ*	0,5069	0,4978 (1;6)	
polη-Ub vs UBZ*	0,2610	1,540 (1;6)	
PIP* vs NLS*	0,0045	19,43 (1;6)	

Table S3. Analysis of xCelligence data. In blue: Corr $CI_{MAX0-50}$: corrected maximum CI recorded in the interval 0-50 h; t_{MAX}: time of appearance of the first maximum; Corr $CI_{MIN30-150}$: corrected minimum CI recorded in the interval 30-150 h; t_{MIN}: time of appearance of minimum CI in the interval 30-150 h. In red: fitted parameters after linear regression of xCelligence data from the interval 0-50 h, after converting CI values to natural logarithms. $t_{1/2\alpha}$: half-life of the first decay phase; $t_{1/2\beta}$: half-life for the second decay phase. In green: fitted parameters after non-linear regression of xCelligence data from the interval 30-150 h using the Boltzmann´s sigmoid equation. t_{50}: time for CI to reach half of its maximal value during the re-growth phase.

ALL CURVES						
	Corr $CI_{MAX0-50}$	**t_{MAX} (h)**	**Corr $CI_{MIN30-150}$**	**t_{MIN} (h)**	**t_{MIN}-t_{MAX} (h)**	**Corr $CI_{MIN30-150}$ ratios (wild-type vs mutants)**
EV	0,4848	15,0953	-0,0857	149,6683		-4,1962
WT	0,5928	19,1286	0,3597	46,4306	27,3020	1,0000
PIP*	0,4149	15,7786	0,0676	65,8006	50,0220	5,3188
NLS*	0,3493	18,8619	0,1017	58,9828	40,1209	3,5381

DEATH PHASE (exponential decay model)				
	$t_{1/2\alpha}$ (h)	**R^2**	**$t_{1/2\beta}$ (h)**	**R^2**
EV	8,6	0,9991		
WT	21,0	0,9965	80,2	0,9454
PIP*	11,3	0,9947	20,8	0,9959
NLS*	11,6	0,9955	25,0	0,9958

RE-GROWTH PHASE (Boltzmann´s sigmoid model)			
	R^2	**t_{50} (h)**	**t_{50}-$t_{MIN30-150}$ (h)**
WT	0,9947	114,9000	68,4694
PIP*	0,9879	187,0000	121,1994
NLS*	0,9882	157,4000	98,4172

Supplemental Experimental Procedures

Molecular cloning

cDNAs encoding for polη, polκ, PCNA and Ub were of human origin. pCDNA3-Flag-polη, pCDNA3-Flag-polη-Ub, pEGFP-C3-polη, pEGFP-C3-polκ, pGEX-4T-2-PCNA, pGEX-4T-1-Ub and pGEX-4T-2-4xUb constructs have been previously described (Bienko et al., 2005; Guo et al., 2008; Guo et al., 2006). pGEX-4T-1-6xHis-Ub was constructed by in-frame insertion of six histidine codons immediately upstream of Ub using site-directed mutagenesis. pEGFP-C3-polη-Ub was prepared in the same way as pCDNA3-polη-Ub. The extra NLS sequence from SV40 large T antigen was inserted into pEGFP-C3 constructs by site-directed mutagenesis using:

5′CTCCTCGCCCTTGCTCACTGGTGGATCTGCTACCTTTCGCTTCTTCTTTGGCATG GTGGCGACCGGTAGC 3′(forward primer);

5′GCTACCGGTCGCCACCATGCCAAAGAAGAAGCGAAAGGTAGCAGATCCACCA GTGAGCAAGGGCGAGGAG 3′ (reverse primer).

pPCAGGFPIP (abbreviated as pCAG elsewhere) was kindly provided by Ian Chambers and the cDNA of NLS-EGFP-polη was cloned in using EcoRI. All the pCAG constructs contained the extra NLS sequence N-terminal to EGFP. All point mutations were introduced using site-directed mutagenesis. The last one hundred-twelve amino acids of polη were cloned into pYTH9 using EcoRI/BglII and into pGEX-4T-1 using EcoRI. In the latter construct the thrombin cleavage site was replaced by the TEV cleavage site. pACT2-PCNA was retrieved from a human thymus library (Clontech) in the course of a yeast two-hybrid screen.

Recombinant proteins

The indicated GST fusions were obtained by inducing transformed *E. coli* BL21 with 0.5 mM IPTG when the culture reached $OD_{600} \approx 0.5$, and growing them for 5 h at 37°C. Bacteria were then harvested in "binding" buffer: 20 mM HEPES [pH 7.5], 150 mM NaCl and 10 μM $ZnCl_2$, supplemented with protease inhibitors prior to use. The bacterial suspension was sonicated, the lysate cleared and passed through a GSTrap™ HP column (GE Healthcare) mounted on an Äktaprime Plus chromatographic system (GE Healthcare). For GST-PCNA, after binding the column was washed with two column volumes of binding buffer containing

1 M NaCl. Elution from the GSTrap™ HP column was performed with binding buffer [pH 8.0] supplemented with 50 mM GSH.

Cell culture and sorting

HEK293T cells were purchased from the American Tissue Culture Collection (ATCC) and grown in DMEM High Glucose medium (GIBCO), supplemented with penicillin (100 U/ml), streptomycin (100 μg/ml) and 10% foetal bovine serum (PAA). SV40-transformed MRC5, XP30RO and XP12RO cells have been described elsewhere (Cleaver et al., 1999; Kannouche et al., 2001; Niimi et al., 2008) and were grown in MEM medium (GIBCO) supplemented with L-glutamine (2 mM), penicillin (100 U/ml), streptomycin (100 μg/ml) and 10% foetal bovine serum. H1299 and H1299Val135 cells were kindly provided by Moshe Oren and grown in RPMI 1640 medium (GIBCO) supplemented with penicillin (100 U/ml), streptomycin (100 μg/ml) and 10% foetal bovine serum.

HEK293T cells were transfected using Lipofectamine Reagent (Invitrogen) according to the manufacturer's instructions. MRC5 and XP30RO cells were transfected using Fugene6 (Roche) according to the manufacturer's instructions. Mock or ATR-specific siRNA (Dharmacon #070108 and #NM001184, respectively) were transfected using Hiperfect (QIAGEN) according to the manufacturer's instructions.

XP30RO cell lines were obtained by transfection of various polη constructs either in pEGFP-C3 or in pCAG, followed by selection in 1 mg/ml G418 or 2 μg/ml of puromycin, respectively. Individual clones were isolated. Upon several passages, XP30RO cell lines containing pEGFP-C3 constructs tended to lose expression of EGFP-polη. To ensure that all the cells used in clonogenic and PRR assays expressed EGFP-polη, the indicated cell lines were sorted immediately prior to use using a BD FACSaria machine (BD Biosciences) to yield a population of cells expressing EGFP-polη at nearly physiological levels. Cell lines containing pCAG constructs, used in the impedance-based measurements, retained stable expression of polη wild-type or mutants after an estimated thirty passages and did not require sorting prior to use (Figure S3B). Importantly, when tested in a clonogenic assay, these cell lines behaved in the same way as the pEGFP-C3 cell lines (data not shown).

Cell lysis

Cells were either lysed in hot Laemmli buffer followed by sonication ("Hot Laemmli" protocol) or in a "Triton" buffer containing 50 mM HEPES [pH 7.5], 150 mM NaCl, 1 mM EDTA, 1 mM EGTA, 1% Triton X-100, 10% glycerol, 25 mM NaF, supplemented with protease inhibitors and 10 mM N-ethylmaleimide (NEM) where indicated. Lysates prepared

with “Triton” buffer were cleared by centrifugation and supernatants were collected. After 5 min boiling proteins were separated by SDS-PAGE.

Triton X-100 extraction

Two different methods were used. In method A, cells on 10 cm dishes were washed with PBS, followed by a wash in CSK buffer (10 mM PIPES [pH 6.8], 100 mM NaCl, 300 mM sucrose, 3 mM $MgCl_2$, 1 mM EGTA, supplemented with protease inhibitors and 10 mM NEM). Next, cells were incubated with 5 ml of the CSK buffer containing 0.2% Triton X-100 for 5 min. The supernatant was collected and precipitated with 25 ml cold acetone to yield the triton-soluble fraction of the cell proteome (TS). The dish was then washed 3 times with the CSK buffer containing 0.02% Triton X-100 and once with PBS. Cell remnants were scraped in “SDS” buffer (50 mM Tris [pH 7.5], 20 mM NaCl, 1 mM $MgCl_2$, 0.1% SDS supplemented with protease inhibitors and 0.25 U/μl benzonase (Novagen)). After 10 min incubation on ice, Laemmli buffer was added to the sample to yield the triton-resistant fraction (TRF). In order to prepare total cell extracts (TCL), boiling Laemmli buffer was added directly on cells. In method B, cells on 10 cm dishes were washed and scraped in PBS. After centrifugation, the pellet was re-suspended in 260 μl PBS and separated into two aliquots, one of 60 μl and one of 200 μl. Both aliquots were centrifuged and the pellet of the 60 μl sample was re-suspended in “SDS” buffer, incubated on ice for 10 min and mixed with Laemmli buffer to yield TCL. The 200 μl sample was re-suspended in CSK buffer containing 0.2% Triton X-100 and incubated on ice for 10 min. This sample was then centrifuged and the supernatant taken to prepare the TS fraction. The pellet was washed once with CSK buffer and re-suspended in “SDS” buffer. After 10 min incubation on ice, Laemmli buffer was added to yield the TRF.

***In vitro* ubiquitination**

Reaction mixtures containing 125 nM E1 (Boston Biochem), 10 μM GST-Ubc5c, 100 μM HIS-Ub, 2.5 mM ATP and the substrate (GST-polη_C) coupled to GSH-Sepharose were incubated for 2 h at 37°C in a reaction buffer (20 mM HEPES [pH 7.5], 150 mM NaCl, 5 mM $MgCl_2$, 50 μM $ZnCl_2$ and 0.05% β-ME). The reaction was stopped by adding Laemmli buffer and boiling it for 5 min. For GST cleavage, TEV protease was added immediately after *in vitro* ubiquitination and incubated for 1 h at 30°C. The reaction was stopped by adding Laemmli buffer and boiling the sample for 5 min.

Mass spectrometry

Protein bands containing Flag-polη conjugated with monoubiquitin were excised from SDS-PAGE gels and subjected to in-gel reduction, alkylation, trypsin digestion and subsequent

sample desalting and concentration, as previously described (Olsen et al., 2004). Digest products were analyzed by nanoLC-MS/MS using an Agilent 1100 nanoflow system connected to an LTQ-FT mass spectrometer (Thermo Fisher Scientific, Bremen, Germany), equipped with a nanoelectrospray ion source (Proxeon Biosystems, Odense, Denmark), as previously described (Olsen et al., 2004). Protein identification and mapping of ubiquitination sites were performed using the Mascot search software (Matrix Science, London, UK).

Laser scanning microscopy

MRC5 cells were grown on coverslips and transfected with Fugene 6. 48-72 h after transfection, cells were washed in PBS and fixed in 2% PFA for 20 min at room temperature. After two washes in PBS, coverslips were mounted on 10 μl of aqueous mounting medium (Biomeda) containing DAPI (Molecular Probes) placed on a glass-holder. Images were acquired using the LSM 510 META laser scanning microscope (ZEISS). For quantification of the percentage of cells with polη, 900 nuclei from three independent experiments were overall scored per each construct.

Yeast two-hybrid system

The library screen was performed as previously described (Bienko et al., 2005). The yeast strain Y190 was transformed as previously described (Hecker et al., 2006) with empty pYTH9 or pYTH9-polη, wild-type or mutants, as baits, and pACT2-PCNA as prey. Yeasts were grown on a synthetic dropout (SD) medium without tryptophan and leucine (SD/-W-L). Colonies appearing after three days on the selection medium were grown overnight in 5 ml of liquid selection medium. 0.5 ml of overnight culture were grown in 4.5 ml of SD/-W-L medium for 1-2 h, the concentration of cells was estimated by measuring the A_{600} and the amount of cells per ml was adjusted by diluting with fresh medium. 5 μl of cell suspension containing the same amount of cells were spotted on SD/-W-L agar plates as well as on 3'AT agar plates. The second day after spotting, cells were transferred to a Whatman filter paper and assayed for β-galactosidase activity with X-gal (5-bromo-4-chloro-3-indolyl-β D-galactopyranoside, Roth).

Curve fitting and statistical analysis

Micrograph quantifications were done using a Student´s T likelihood two-tails test.

When appropriate, differences between curves from the clonogenic assay or the xCelligence system were analysed using the likelihood F test.

Clonogenic assay: for each cell line, the logarithm of the number of clones (expressed as percent of the 0-dose value) was plotted against the UV dose and data points were fitted to the equation:

$$Ln\left[Cl_{\%}\right] = Ln\left[Cl_{\%0}\right] - k \cdot D \qquad (1)$$

using GraphPad Prism software. $Cl_{\%}$ represents the percent of clones surviving after each dose D, $Cl_{\%0}$ the value at 0-dose and k the slope of the line. Doses resulting in 50% survival were obtained from the slopes of fitted curves as:

$$D_{50} = \frac{Ln2}{k} \qquad (2)$$

Data obtained with the xCelligence system were first visually inspected to obtain several parameters ($CI_{MAX0\text{-}30}$, first CI maximum; t_{MAX}, time of the appearance of the first maximum; $CI_{MIN30\text{-}150}$, minimum reached by CI; t_{MIN}, time at which minimum is reached). Each of these parameters values was then corrected by a factor C equal to $\frac{CI_{WT}}{CI_{MUT}}$, where CI_{WT} is the average CI at 20 h obtained in wild-type cells from two independent experiments without UV damage and CI_{MUT} the corresponding value in mutant cell lines (EV, PIP*, NLS*). This correction may control for morphological and behavioral differences observed between different cell lines (data not shown). Subsequently, the decay phase after the first CI maximum and the lagged re-growth phase observed for all cell lines except the EV control were modeled separately. For the decay phase, natural logarithms of CI values between the first maximum and the minimum were plotted against time and the linear regions of the obtained curves were fit by GraphPad to an equation similar to (1):

$$Ln\left[CI\right] = Ln\left[CI_0\right] - k \cdot t \qquad (3)$$

where CI_0 is the curve intercept for t=0 and t represents time. Half-life values were calculated for each fitted curve as: $t_{1/2} = \frac{Ln2}{k}$. To model the CI profile over time in untreated cells and in UV-treated cells during the re-growth phase, curves were fitted using GraphPad to the Boltzmann sigmoid equation:

$$CI = CI_{MIN} + \frac{(CI_{MAX} - CI_{MIN})}{(1 + e^{\frac{t_{50} - t}{k}})} \qquad (4)$$

where CI_{MIN} and CI_{MAX} represent the CI value at the beginning and at the end of the growth phase, respectively; t_{50} is the time required for CI to reach half of CI_{MAX}; k is the slope of the curve; t is time.

Supplemental References

Cleaver, J.E., Afzal, V., Feeney, L., McDowell, M., Sadinski, W., Volpe, J.P., Busch, D.B., Coleman, D.M., Ziffer, D.W., Yu, Y.*, et al.* (1999). Increased ultraviolet sensitivity and chromosomal instability related to P53 function in the xeroderma pigmentosum variant. Cancer Res *59*, 1102-1108.

Hecker, C.M., Rabiller, M., Haglund, K., Bayer, P., and Dikic, I. (2006). Specification of SUMO1- and SUMO2-interacting motifs. J Biol Chem *281*, 16117-16127.

Niimi, A., Brown, S., Sabbioneda, S., Kannouche, P.L., Scott, A., Yasui, A., Green, C.M., and Lehmann, A.R. (2008). Regulation of proliferating cell nuclear antigen ubiquitination in mammalian cells. Proc Natl Acad Sci U S A *105*, 16125-16130.

Olsen, J.V., Ong, S.E., and Mann, M. (2004). Trypsin cleaves exclusively C-terminal to arginine and lysine residues. Mol Cell Proteomics *3*, 608-614.